

NAVAL POSTGRADUATE SCHOOL MONTEREY, CALIFORNIA



THESIS

COMPARISON OF A PIN STACK TO A CONVENTIONAL STACK IN A THERMOACOUSTIC PRIME MOVER

by

F. Scott Nessler

December, 1994

Thesis Advisor:

Robert M. Keolian

Approved for public release; distribution is unlimited.

19950517 063

DTIC QUALITY INSPECTED 5

REPORT DOCUMENTATION PAGE			Form Approved OMB No. 0704-0188	
Public reporting burden for this collection of information is estimated to average 1 hour per response, including the time for reviewing instruction, searching existing data sources, gathering and maintaining the data needed, and completing and reviewing the collection of information. Send comments regarding this burden estimate or any other aspect of this collection of information, including suggestions for reducing this burden, to Washington Headquarters Services, Directorate for Information Operations and Reports, 1215 Jefferson Davis Highway, Suite 1204, Arlington, VA 22202-4302, and to the Office of Management and Budget, Paperwork Reduction Project (0704-0188) Washington DC 20503.				
1. AGENCY USE ONLY (Leave blank)	2. REPORT DATE December 1994	3. REPORT TYPE AND DATES COVERED Master's Thesis		
4. TITLE AND SUBTITLE COMPARISON OF A PIN STACK TO A CONVENTIONAL STACK IN A THERMOACOUSTIC PRIME MOVER		5. FUNDING NUMBERS		
6. AUTHOR(S) Nessler, F. Scott				
7. PERFORMING ORGANIZATION NAME(S) AND ADDRESS(ES) Naval Postgraduate School Monterey CA 93943-5000		8. PERFORMING ORGANIZATION REPORT NUMBER		
9. SPONSORING/MONITORING AGENCY NAME(S) AND ADDRESS(ES) Office of Naval Research ONR 331 800 North Quincy Street Arlington VA 22217-5660		10. SPONSORING/MONITORING AGENCY REPORT NUMBER		
11. SUPPLEMENTARY NOTES The views expressed in this thesis are those of the author and do not reflect the official policy or position of the Department of Defense or the U.S. Government.				
12a. DISTRIBUTION/AVAILABILITY STATEMENT Approved for public release; distribution is unlimited.		12b. DISTRIBUTION CODE		
13. ABSTRACT (maximum 200 words) This thesis compares the pin stack with a conventional rolled stack for a thermoacoustic prime mover. A pin stack is a new geometry for stacks used in thermoacoustic engines consisting of a lattice of small wires which are spaced about a thermal penetration depth apart. Computer simulations were conducted on a variety of pin stack geometries and operating parameters. Results indicate that the modeling program, DeltaE, agrees with the experimental results for conventional stacks, that the pin stack decreases viscous energy losses, and greatly increases the efficiency of the thermoacoustic engine over a large range of mean pressures. The pin stack performance was found to be more sensitive than the conventional stack to changes in thermal and viscous penetration depths of the fluid.				
14. SUBJECT TERMS Thermoacoustic, Pin Stack, Refrigeration		15. NUMBER OF PAGES 64		
		16. PRICE CODE		
17. SECURITY CLASSIFICATION OF REPORT Unclassified	18. SECURITY CLASSIFICATION OF THIS PAGE Unclassified	19. SECURITY CLASSIFICATION OF ABSTRACT Unclassified	20. LIMITATION OF ABSTRACT UL	

Approved for public release; distribution is unlimited.

COMPARISON OF A PIN STACK TO A CONVENTIONAL STACK IN A
THERMOACOUSTIC PRIME MOVER

by

F. Scott Nessler
Lieutenant, United States Navy
B.S., University of Illinois, 1988

Submitted in partial fulfillment
of the requirements for the degree of

MASTER OF SCIENCE IN APPLIED PHYSICS

from the

NAVAL POSTGRADUATE SCHOOL

December 1994

Author:

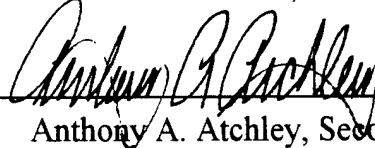


F. Scott Nessler

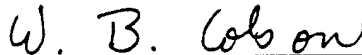
Approved by:



Robert M. Keolian, Thesis Advisor



Anthony A. Atchley, Second Reader



William B. Colson, Chairman
Department of Physics

Accession For	
NTIS	CRA&I <input checked="checked" type="checkbox"/>
DTIC	TAB <input type="checkbox"/>
Unannounced <input type="checkbox"/>	
Justification	
By	
Distribution /	
Availability Codes	
Dist	Avail and/or Special
A-1	

ABSTRACT

This thesis compares the pin stack with a conventional rolled stack for a thermoacoustic prime mover. A pin stack is a new geometry for stacks used in thermoacoustic engines consisting of a lattice of small wires which are spaced about a thermal penetration depth apart. Computer simulations were conducted on a variety of pin stack geometries and operating parameters. Results indicate that the modeling program, DeltaE, agrees with the experimental results for conventional stacks, that the pin stack decreases viscous energy losses, and greatly increases the efficiency of the thermoacoustic engine over a large range of mean pressures. The pin stack performance was found to be more sensitive than the conventional stack to changes in thermal and viscous penetration depths of the fluid.

TABLE OF CONTENTS

I. INTRODUCTION	1
II. THEORY	3
III. COMPUTER SIMULATIONS	11
A. COMPUTER SIMULATIONS FOR THE DESIGN OF A PIN STACK	11
1. Conventional Stack Simulation	11
2. Computer Design of a Pin Stack	14
B. COMPARISON OF PIN STACK TO CONVENTIONAL STACK	19
1. Varying Pressures	22
2. Onset	22
3. Efficiency	22
4. Hysteretic Effects	26
C. COMPUTER SIMULATIONS OF THE PROPOSED STACK	29
IV. CONSTRUCTION OF THE PIN STACK	33
A. CREATION OF PIN STACK SHELL	33
1. Cutting The Heat Exchanger Notches	33
2. Heat Exchanger Holders	33
3. Insertion Of Glass	34
4. Initial Low Temperature Test	34
5. Addition Of Teflon Seals	34
6. Second Low Temperature Test	35
B. THREADING THE PINS BY HAND	35
V. CONCLUSIONS	37

APPENDIX A. INPUT FILE FOR CONVENTIONAL STACK	39
APPENDIX B. INPUT FILE FOR PIN STACK	43
APPENDIX C. INPUT FILE FOR ACTUAL PIN STACK	47
APPENDIX D. DRAWINGS FOR PIN STACK MANUFACTURE	51
LIST OF REFERENCES	53
INITIAL DISTRIBUTION LIST	55

ACKNOWLEDGEMENT

The author would like to acknowledge the financial support of the Office of Naval Research, performed under Contract N0001495WR2001 and N0001494WR23044.

I. INTRODUCTION

Thermoacoustic engines are divided into two categories: prime movers and heat pumps. In thermoacoustic heat pumps, high amplitude acoustic standing waves pump heat along the boundary of a solid, typically a stack or roll of plates generically called a "stack," situated in the standing wave. The acoustically generated heat flow produces a thermal gradient along the stack. Thus, acoustic energy is converted into stored thermal energy.

Prime movers operate with the reciprocal process; heat flows through the engines from high to low temperature. The stack provides a stored thermal gradient which then causes the air in the tube to vibrate and generate acoustic waves. In order to produce sound, the vibrational energy must overcome the energy dissipated by losses within the prime mover. Primary loss mechanisms are thermal and viscous losses along the surfaces of the tube walls, stack, and heat exchangers on either side of the stack. The apparatus achieves "onset" when it starts to produce sound.

The main purpose of this thesis is to determine whether the use of a new type of stack construction, the pin stack (Swift, 1993), will increase the efficiency of a prime mover. In a pin stack, the solid is in the form of an array of pins or wires, rather than flat sheets. Simulations were performed using both a conventional rolled stack and the pin stack in a particular example of a prime mover, which consists of a half wave tube, two heat exchangers, hot and cold, in thermal contact with a replaceable stack (Castro, 1993). The section below the cold heat exchanger is submerged in liquid nitrogen, and the portion above the hot exchanger is held at ambient temperature. This creates a temperature gradient across the stack which produces acoustic energy. Data from the previously conducted experiment will be compared to results generated by computer simulation using the program DeltaE (Ward, 1994). While these simulations are only intended to compare the pin stack in a given system, it is believed that the results will be indicative to other prime movers and in the more complex refrigerator systems.

II. THEORY

In this section a brief review of the theory behind prime movers and the important role of the stack is made. This is a summary of the arguments and descriptions given in the article "Thermoacoustic Engines" by G.W. Swift (1988).

To examine the basic principles involved in the thermoacoustic engine and the role of the stack, Swift first discusses a simple example in which the acoustic and thermodynamic effects are nearly distinct. If the fluid moving about a plate oriented parallel to the direction of a standing wave is examined, two effects can be observed: a time-averaged heat flux near the surface of the plate along the direction of the acoustic wave, and the generation or absorption of acoustic power near the surface of the plate.

It is already known that in the absence of the plate the standing wave is nearly adiabatic and that there is an oscillating temperature that is dependent on the amplitude of the pressure oscillations. This change in temperature is in phase with the change in pressure. The general form for ideal gases is

$$\frac{T_1}{T_m} = \frac{\gamma - 1}{\gamma} \frac{p_1}{p_m}, \quad (1)$$

where T_1 and p_1 are the oscillating components and T_m and p_m are the mean components of the temperature and pressure, respectively, and γ is the ratio of isobaric to isochoric specific heats. For monatomic ideal gases $\gamma = 5/3$.

If a plate is now inserted into the flow, the original temperature oscillations are modified in both magnitude and phase for fluid that is about a thermal penetration depth away from the plate. Thermal penetration depth is defined as

$$\delta_\kappa = \sqrt{2\kappa/\omega}, \quad (2)$$

where $\kappa = K/\rho_m c_p$, K is the thermal conductivity, ρ_m is the mean density, and c_p is the isobaric heat capacity per unit mass of the fluid. The thermal penetration depth is roughly the distance that heat can diffuse through the fluid during a time $2\pi/\omega$.

Swift calculates T_1 , the oscillating temperature, from the general equation of heat transfer and using the following assumptions: the plate is much shorter than a wavelength and far enough away from pressure or velocity nodes so that p_1 and u_1 can be considered uniform over the plate, the fluid has zero viscosity so that u_1 does not depend on y , the plate has a constant temperature gradient ∇T_m along the x direction, and that the mean fluid temperature is independent of y , where the x direction is the direction of the flow of the fluid and y is the perpendicular distance from the plate. His calculations lead to the result,

$$T_1 = \left(\frac{T_m \beta}{\rho_m c_p} p_1 - \frac{\nabla T_m}{\omega} u_1 \right) (1 - e^{-(1+i)y/\delta_\kappa}) , \quad (3)$$

where β is the thermal expansion coefficient of the fluid. Since fluid far from the plate makes negligible thermal contact to the plate, for $y \gg \delta_\kappa$ the expression simplifies to,

$$T_1 = \frac{T_m \beta}{\rho_m c_p} p_1 - \frac{\nabla T_m}{\omega} u_1 . \quad (4)$$

The first term is due to the adiabatic process as described in Eq. 1. The second term comes from the mean temperature gradient of the fluid. As the fluid particle oscillates across the plate, the temperature at a point in space changes by an amount $(\nabla T_m u_1)/\omega$ even if each fluid particle temperature remains constant. From Eq. 3 we can define a ∇T_{crit} such that these two effects balance and $T_1 = 0$. This is called the critical temperature gradient. The critical temperature gradient is important because it is the boundary between the prime mover and the heat pump functions of thermoacoustic engines.

Examination of Eq. 3 reveals that the y dependent part of T_1 is complex. For small y , $y \ll \delta_\kappa$, the exponential term goes to 1 indicating $T_1 = 0$, no fluctuation in temperature. For large y , the y dependence vanishes indicating that temperature fluctuations depend only on x . However, when $y \sim \delta_\kappa$ there is a large imaginary part to T_1 that is out of phase with the adiabatic temperature fluctuations but in phase with the velocity. This phase shift leads directly to time averaged heat flux in the x direction.

Swift then derives heat flux, work flux, and efficiency. The derivation is not critical to this thesis but much can be gained by looking at the results. The total heat flux \dot{Q} is given by

$$\dot{Q} = -\frac{1}{4}\Pi\delta_x T_m \beta p_1 u_1 (\Gamma - 1) , \quad (5)$$

where Π is the perimeter of the plate and $\Gamma = \nabla T_m / \nabla T_{crit}$. For ideal gases $T_m \beta = 1$. The heat flux is proportional to the area, $\Pi\delta_x$, the product of $p_1 u_1$, and the temperature gradient through the term $\Gamma - 1$. Since the product $p_1 u_1 = 0$ at either a pressure or velocity node, there is no heat flux at these points in a standing wave. Likewise, no heat flux occurs when $\nabla T_m = \nabla T_{crit}$ because $\Gamma - 1 = 0$.

In a similar fashion, an expression for the work flux, or acoustic power, is derived:

$$\dot{W} = \frac{1}{4}\Pi\delta_x \Delta x \frac{T_m \beta^2 \omega}{\rho_m c_p} (p_1)^2 (\Gamma - 1) . \quad (6)$$

This expression is quite similar to that of heat flux. The work flux is proportional to the volume of air that is about a thermal penetration depth from the plate, $\Pi\delta_x \Delta x$, and the work flux vanishes at pressure nodes as indicated by $(p_1)^2$. If $(\Gamma - 1) > 0$, work is done on the fluid and the engine is a prime mover. Work is removed from the fluid if $(\Gamma - 1) < 0$ and the engine becomes a heat pump.

Efficiency η for a prime mover is defined as the ratio of the work flux to the heat flux. Manipulation and algebra reveals that $\eta = \eta_c / \Gamma$, where η_c is the Carnot efficiency, the maximum possible efficiency of an engine with the same temperature gradient over the same distance. The thermoacoustic engine is most efficient as $(\Gamma - 1) \rightarrow 0$ i.e. $\nabla T_m \rightarrow \nabla T_{crit}$. However Eq. 6 reveals little power is produced for $\Gamma \approx 1$. Likewise, for large power output the efficiency of the engine is low. This shows a characteristic trade-off between power and efficiency.

To expand this simplified view and look at a more realistic thermoacoustic engine, a stack must be added to interact with the fluid and the effects of viscosity must be taken into

account. The easiest stack to examine is the conventional rolled stack which can be viewed as several flat plates stacked upon each other. These factors modify the above equations leading to this result for acoustic power:

$$\dot{W} = \frac{1}{4} \Pi \delta_{\kappa} \Delta x \frac{(\gamma-1)\omega(p_1)^2}{\rho_m a^2 (1+\epsilon_s)} (\Gamma-1) - \frac{1}{4} \Pi \delta_v \Delta x \omega \rho_m \langle u_1 \rangle^2, \quad (7)$$

where a denotes the speed of sound. The first term in this expression is the same as Eq. 6, the simple plate without viscosity, with the exception of the term $1/(1+\epsilon_s)$ where $\epsilon_s = \rho_m c_p \delta_{\kappa} / \rho_s c_s \delta_s$, where for the solid, ρ_s , c_s , and δ_s are the density, heat capacity per unit mass, and the thermal penetration depth, respectively. This factor takes into account the heat capacity of the plate within a thermal penetration depth of the surface. If the plate does not have a large heat capacity compared to the fluid then the boundary condition of $T_1=0$ will not be met and the acoustic power will be lessened. The second term in Eq. 7 shows the effects of viscosity of the fluid. This is also a volume dependent quantity, the volume of air within a viscous penetration depth of the fluid, and is dependent on the average velocity of the fluid particle squared. This is the power dissipated by viscous shear of the fluid against the plate. It is through these competing volumes, $\Pi \delta_{\kappa} \Delta x$ and $\Pi \delta_v \Delta x$, in the acoustic power that the pin stack makes an improvement. Since the penetration depths are competing factors, it would be beneficial to more closely examine the thermal and viscous effects. Both effects are functions of y , perpendicular from the plate but in different ways.

The thermal effects are proportional to the term

$$Im[-e^{-(1+i)y/\delta_{\kappa}}] \quad (8)$$

The graph of this term, Fig. 1, reveals that 80% of the thermal effects occur between $0.4\delta_{\kappa}$ and $1.91\delta_{\kappa}$, with the maximum effects around δ_{κ} away from the plate. (Swift, 1993) However, the viscous effects are proportional to the term

$$e^{-2y/\delta_v} \quad (9)$$

A graph of this term, Fig. 2, shows that 80% of the viscous effects occur within $0.8\delta_v$ of the surface of the plate (Swift, 1993). For neon at 310 K the following values apply: $\delta_k=6.5\times 10^{-4}$ m and $\delta_v=5.3\times 10^{-4}$ m. Figure 3 plots Eq. 8 and 9 for these values and marks the appropriate 80% range. Clearly these effects occur at different locations and over different ranges from the plate. This implies that the shape of the plate could effect the acoustic power generated. If some way could be found to decrease the viscous area compared to the thermal area, the acoustic power for given penetration depths would be increased and result in the increase of the efficiency.

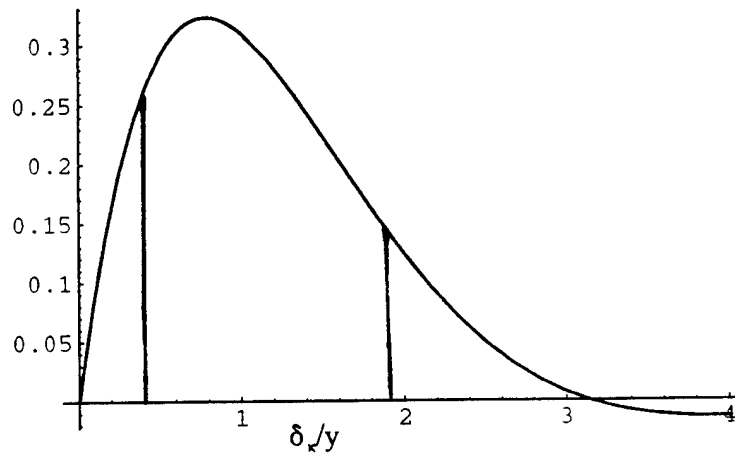


Figure 1. Thermal effects.

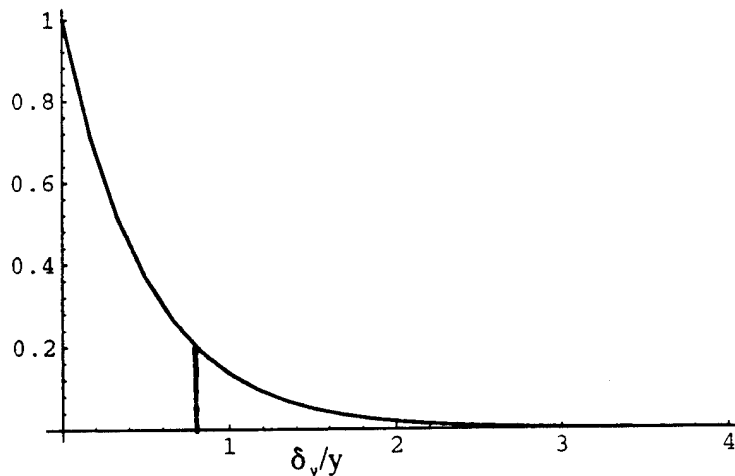


Figure 2. Viscous effects.

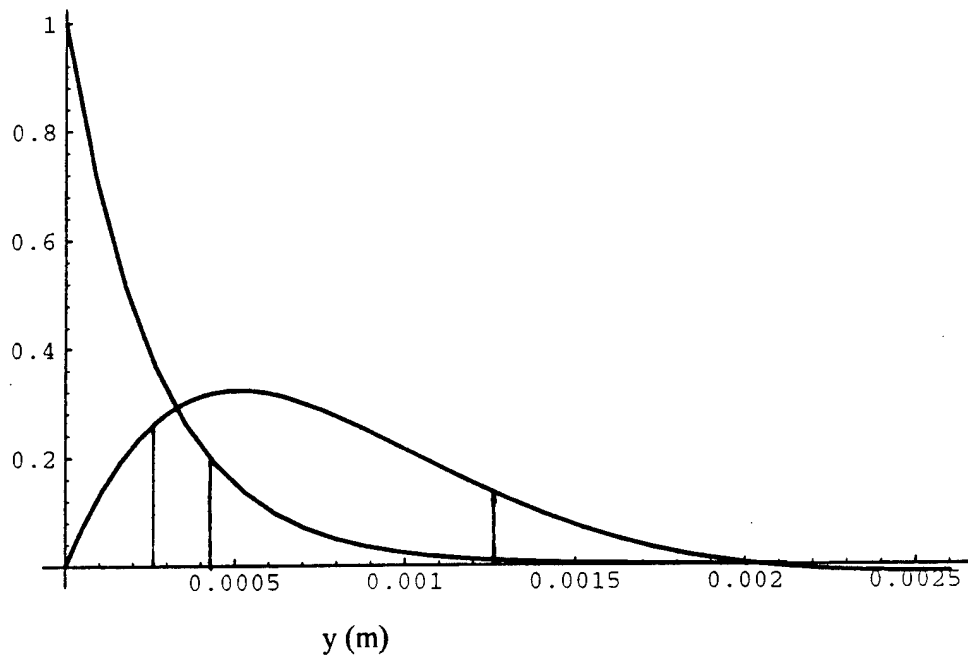


Figure 3.Viscous and thermal effects at 310 K for neon.

If an arbitrary value for δ_v and δ_x with $\delta_x > \delta_v$ is chosen, and with the assumption of an infinitely small pin, a simple geometric argument can be made to show the advantage of the pin to that of a plate. Figure 4 shows such a setup for the pin and plate.

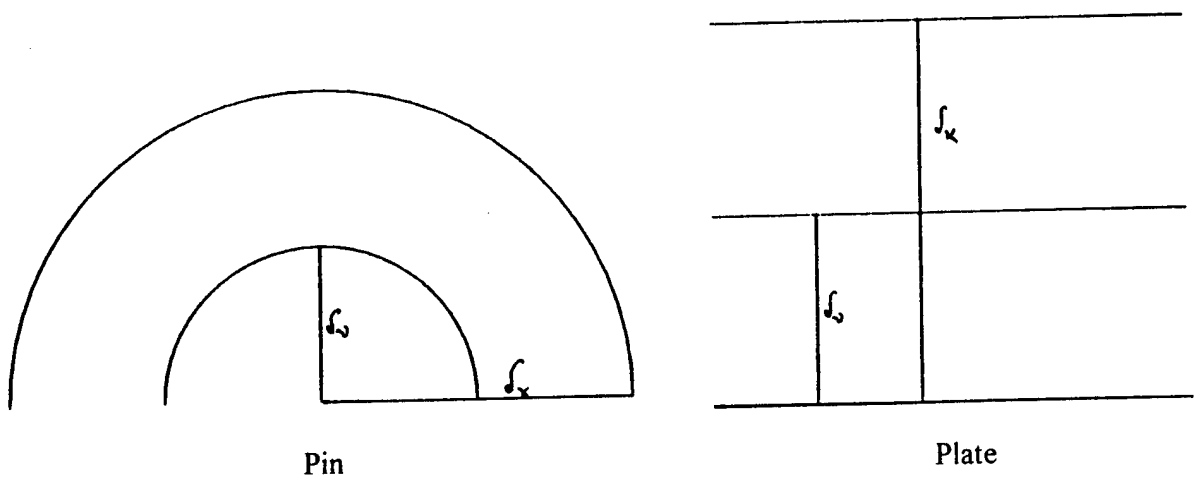


Figure 4. Pin and plate dependence on penetration depths.

The ratio of thermal area to viscous area is proportional to δ_x/δ_v for the plate and $(\delta_x/\delta_v)^2$ or as the radius squared for the pin. Comparing the pin and plate ratios show that the pin improves thermal to viscous areas by an extra factor of δ_x/δ_v . While this is an overly simplified argument and does not take into account differences in the y dependence of the thermal and viscous work terms for cylindrical versus planer geometries, and other important details, as discussed in the paper by Swift (1993), it does imply that the shape of the surfaces in the stack could influence the performance and that the convex surface may perform better than that of a flat plate.

The effect is enhanced when the difference between the penetration depths is increased. Since δ_x and δ_v are fluid and temperature dependent properties, the choice of the fluid is extremely important when trying to optimize the efficiency of a thermoacoustic engine. Also an increase in the curvature leads to improved efficiency. This would lead a designer to use arbitrarily small pins, however, so ϵ_s must also be considered. If the pins become too small the heat capacity of the pins will not be large enough to impose the $T_1=0$ boundary condition and the efficiency will be decreased. (Swift, 1988) In addition, in order to create the most acoustic power, the arrangement of the pins is also important. The spacing between pins should not be much more than $2\delta_x$, because of the reduced thermal effects. The pins should be arranged in a hexagonal lattice to allow for the most pins with equal spacing. While these are optimum conditions, the exact spacing between the pins is not expected to be critical due to the large range over which the thermal effects occur.

III. COMPUTER SIMULATIONS

The primary goal of this thesis is to compare the performance of a pin stack to that of the conventional stack and verify computer modeling of the pin stack by DeltaE. DeltaE is a computer program for modeling and designing thermoacoustic and other one-dimensional acoustic apparatus. DeltaE numerically integrates a one-dimensional wave equation in the usual acoustic approximation through a series of segments, such as ducts and heat exchangers. It uses continuity of oscillating pressure, oscillating volumetric velocity, and mean temperature to match the solutions of adjacent segments. The iteration is controlled by global variables such as frequency and mean pressure and by local variables such as the geometry of a segment and enthalpy flow. DeltaE is very versatile due to the large range of boundary conditions the user can set. By identifying a series of inputs, global variables or guesses, and the desired outputs, known as targets and boundary conditions, the problem is solved iteratively; guesses are varied until targets are reached. When the solutions and boundary conditions agree with what is desired, the solution is said to converge. The user can set the error tolerances for matching targets. (Ward, 1994) Simulations were run using an Intel Pentium processor which has been recently reported to show errors in some computers when doing math intensive operations, however, it is not known if this processor has adversely effected the simulations.

A. COMPUTER SIMULATIONS FOR THE DESIGN OF A PIN STACK

1. Conventional Stack Simulation

To make an accurate comparison of the pin stack to that of a conventional rolled stack, a thermoacoustic prime mover for which experimental data was available was used. This prime mover, described in detail in "Experimental Heat Exchanger Performance in a Thermoacoustic Prime Mover" by Nelson C. Castro (1993), was used to evaluate the influence of different types of heat exchangers at varying mean pressures. Figure 5 shows the prime mover used in these experiments. Notice that the lower portion of the drawing is not to scale in order to give a better scale for the shorter sections. A constant temperature gradient was created by placing a heater collar around the upper heat exchanger

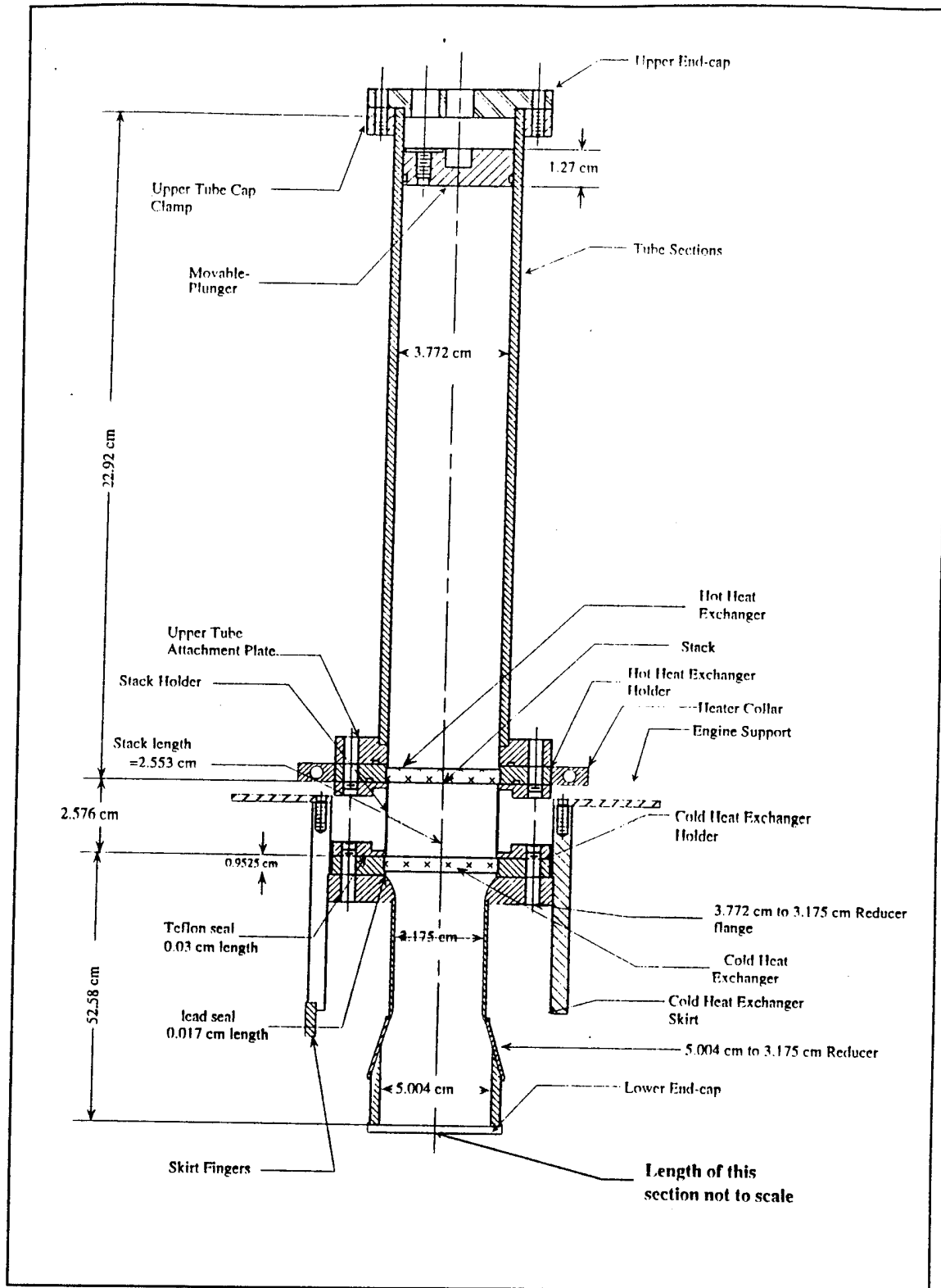


Figure 5. Prime mover (Castro, 1993).

and immersing the lower tube in liquid nitrogen. The data by Castro with this prime mover was compared to predictions of DeltaE to ensure proper modeling.

It was desired to model the conventional stack with the environment and dimensions similar to that which will be used with the pin stack, specifically a 0.82 cm heat exchanger and operating pressure of 27.6 kph in neon. The thickest of three heat exchangers used by Castro was chosen for practical manufacturing reasons. Since the pins, or wires, were expected to be strung between the two heat exchangers and kept under tension, there was a concern that the thinner heat exchanger fins might buckle under the combined strain of the two thousand plus wires. In addition, the idea of cutting notches or grooves in the heat exchanger fins to hold the wires in place was being considered and the thicker heat exchangers would provide the flexibility for these types of ideas. While the stronger structure was desired for construction, the additional surface of the larger fins could effect the data if the viscous effects of the stack are dominated by the heat exchanger.

An input file for DeltaE was constructed using the description of the thermoacoustic prime mover from Castro's thesis. A few adjustments to the actual geometry had to be made for the simulation since the lower section of the apparatus is kept at temperature by immersion in liquid nitrogen. The DeltaE program prefers that all of the radial heat flow occur at the heat exchangers, so the radial heat flow in the lower tube is more difficult to model. DeltaE does allow for some radial heat flow in sections it calls stack ducts but in these the temperature gradient of the fluid must be well known to model correctly (Ward, 1993). Since the temperature profile in the lower tube is not accurately known and changes according to the work produced by the engine, this problem was dealt with by making the lower section longer. The lengthening of the lower section has the same effect on the frequency as lowering the temperature of the gas in this section. The lower section was lengthened by 33% and no attempt was made to maintain the surface area of the tube. Having the correct frequency for the prime mover is important if the stack performance is to be properly modeled.

DeltaE simulations were run with the metal temperatures fixed for the hot end of the pins and the cold heat exchanger at 310 K and 106 K respectively, and the velocity was

required to go to zero at the bottom end of the tube. The frequency, mean temperature of the fluid at the top end, heat provided to the engine at the hot exchanger and the acoustic output were allowed to vary. The mean pressure was held at 27.6 kph. The program was run several times, the length of the lower section was changed after each iteration to match the frequency observed in the experimental data, 166 Hz. Once this frequency matching was completed, the simulation giving the value of 167 Hz, the acoustic pressure amplitude generated was compared between the computer model and the experiment. The computer model generated a 7.47 kph acoustic pressure while the actual data gave 7.07 kph. This was considered to be a close enough match to insure good computer modeling for this engine at 27.6 kph. The agreement between the simulation and experiment is a bit surprising because it depends on DeltaE accurately modeling thermal contact between the gas and the heat exchangers.

2. Computer Design of a Pin Stack

With the successful modeling of the conventional stack, the next step was to design a pin stack to be used in the prime mover. DeltaE input conditions were the same as described above. The program was set up to vary the pin spacing for a given pin radius. The pin sizes were chosen from those commercially available, 1, 2, 3, 5, and 10 thousandths of an inch diameter constantan wire. Since constantan wire is not one of the options in DeltaE, stainless steel was modeled instead. The thermal properties of these two metals are similar. After the program was run the results were tabulated and trends examined.

For each pin size, there was an optimum spacing that produced the highest efficiency, acoustic pressure, and stack work. Figure 6 shows the acoustic pressure and Fig. 7 shows the stack work for the various pin diameters and spacings. The optimum spacing for acoustic amplitude did not coincide with the optimum spacing for stack work. Efficiency relative to Carnot is defined here as

$$\frac{\text{Stack Work}}{\text{Heat In}} \left(\frac{T_h}{T_h - T_c} \right), \quad (10)$$

where T_h is the temperature of the stack pins close to the hot exchanger, T_c the temperature of the pins near the cold exchanger, Stack Work the amount of work produced by the stack,

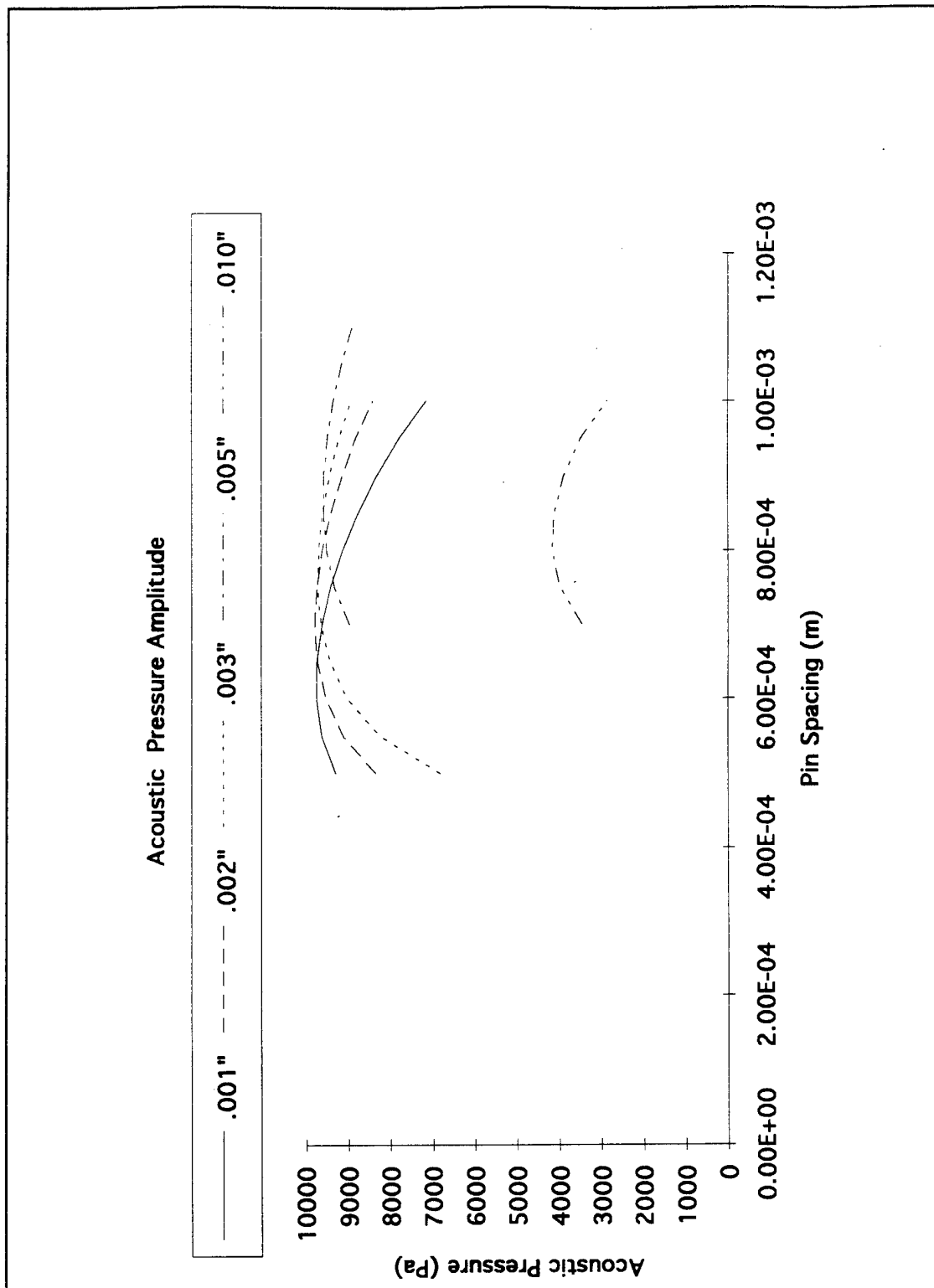


Figure 6. Acoustic pressure amplitude as a function of pin spacing for various pin diameters.

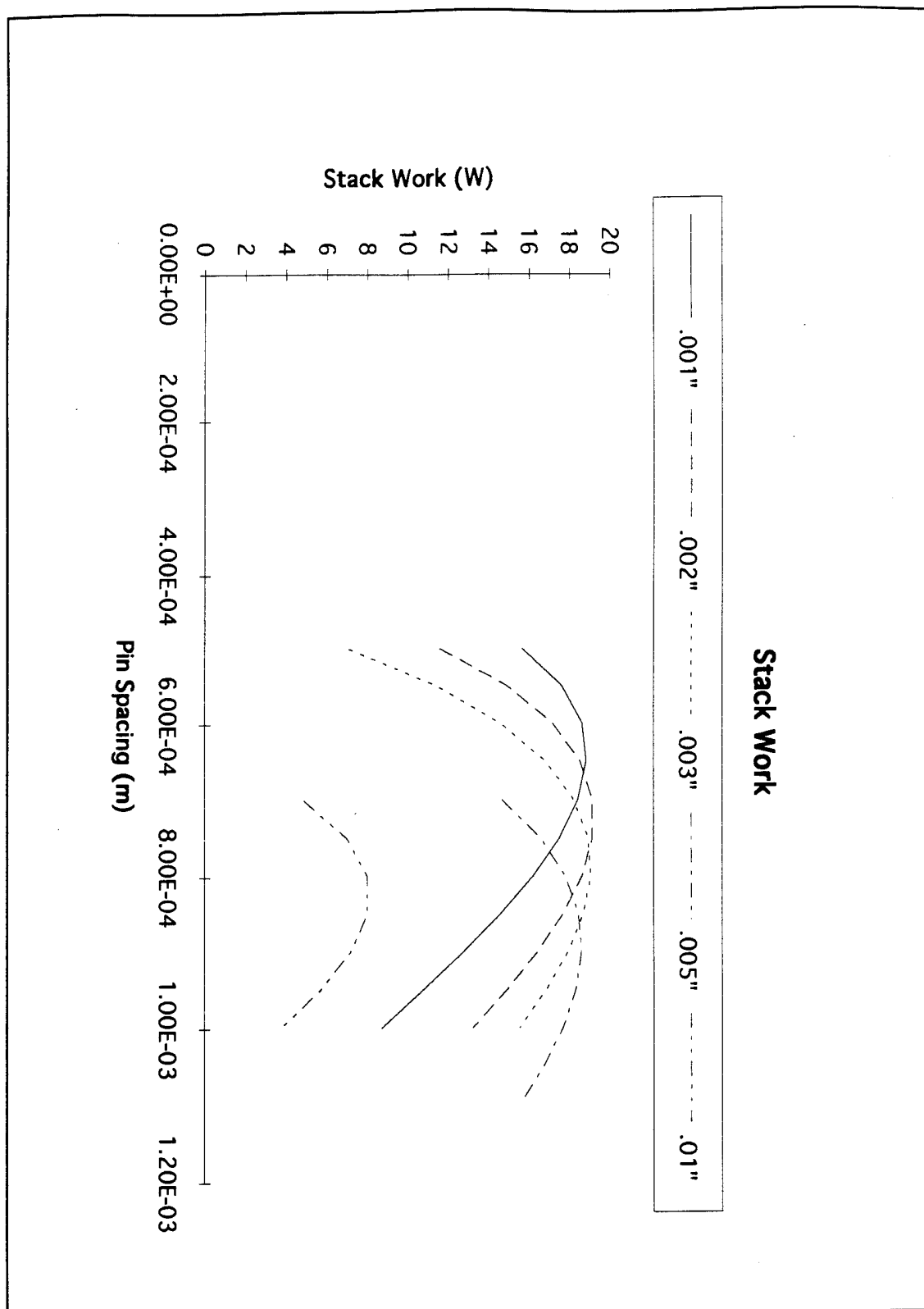


Figure 7. Stack work as a function of pin spacing for various pin diameters.

and Heat In the amount of heat that was put into the apparatus at the hot exchanger. Figure 8 is a plot of the efficiency vs pin spacing for a variety of pin diameters.

As the pin size increased, the peak efficiency of the thermoacoustic engine decreased and likewise the amount of sound produced was less. This is as expected from the intuitive picture presented earlier. The smaller the pin radius the higher the curvature of the surface and the bigger the desired effect of decreasing viscous to thermal volumes. This would lead to designing infinitely small pins but, as discussed before, the designer must also consider the heat capacity of the metal and insure that ϵ_s remains small.

The expression for ϵ_s for the pins is not as simple or straightforward as that of the plate since it involves Bessel functions and Rott's function f_κ . For pins,

$$\epsilon_s = \left(\frac{K \rho c_p}{K_s \rho_s c_s} \right)^{\frac{1}{2}} \frac{J_0(\sqrt{-i\omega/\kappa_s} r_i)}{J_1(\sqrt{-i\omega/\kappa_s} r_i)} f_\kappa \sqrt{-\frac{i\omega(r_o^2 - r_i^2)}{\kappa 2r_i}}, \quad (11)$$

where the subscript s refers to the solid properties, r_i is the pin radius and r_o is related to the pin spacing by $r_o = \sqrt{2\sqrt{3}/\pi} y_0$ where $2y_0$ is the distance between pins in a hexagonal lattice.

(Swift, 1993) When calculated for the smallest pin size, the magnitude of ϵ_s was .0107, still a relatively small number.

All of these results supported what is currently suspected about pin stacks. The .003" wire was chosen to be used to build the pin stack. While the efficiency of the .003" is slightly less than that of the .001" or .002" wire, the larger wire should be easier to work with and pose less problems of breaking while constructing the pin stack. The optimum spacing was initially chosen by DeltaE. The optimum pin spacing for the maximum efficiency with the .003" wire, 33.92% Carnot, was 800 μm .

It was decided that the pins would somehow be attached to the copper fins of the heat exchangers and so different heat exchangers than those used in Castro's experiment had to be manufactured. Heat exchanger were made with material provided by Jay Adeff and Tom

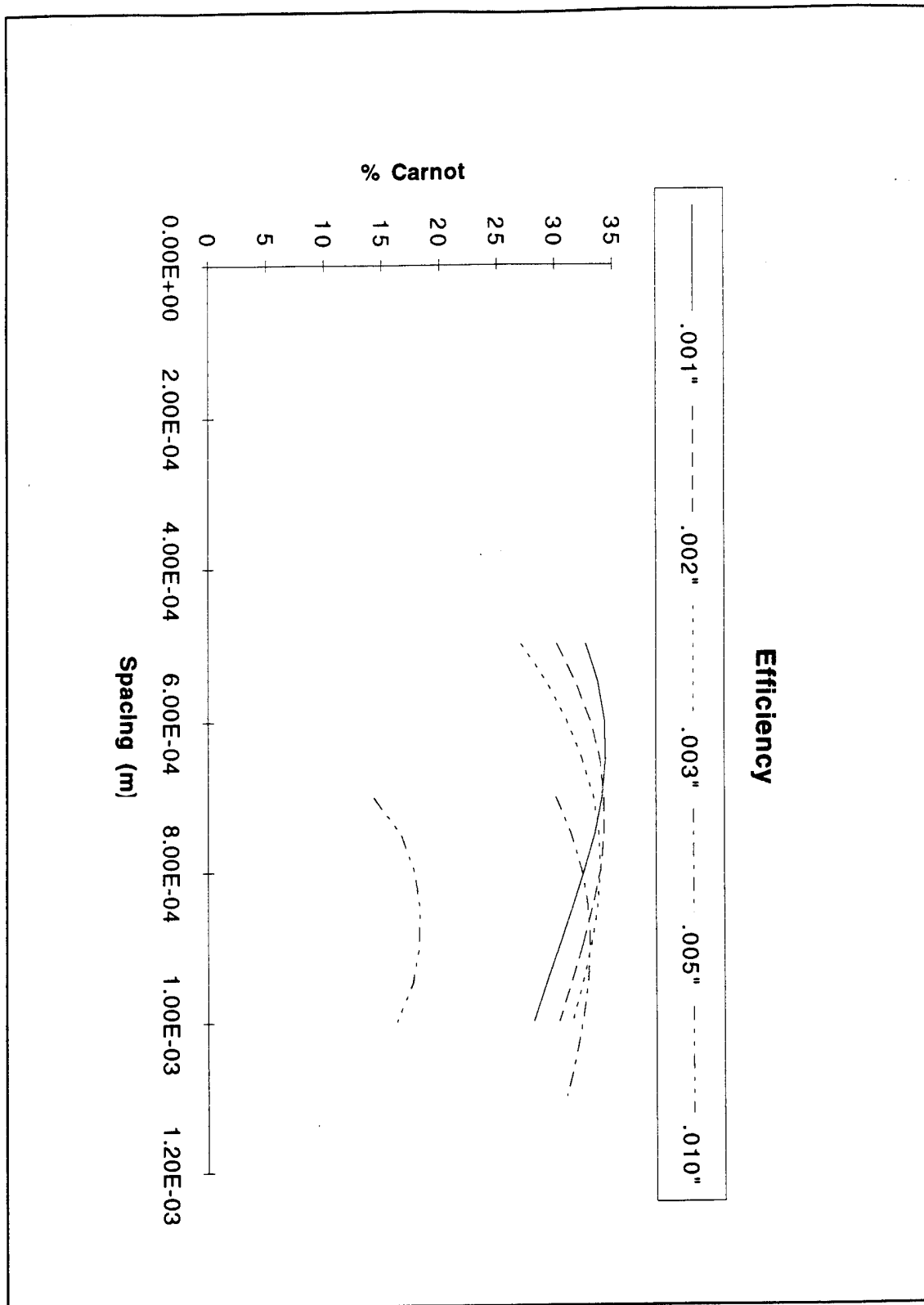


Figure 8. Efficiency as a function of pin spacing for various pin diameters.

Hofler of the Naval Postgraduate School. The final dimensions were: width along acoustic axis of .82 cm, outside radius of 1.89 cm, fins 230 μm thick, center to center spacing of 746.8 μm . These dimensions closely resemble those of Castro's experiment. A nearly hexagonal lattice of pins can be sewn onto these heat exchangers, as shown in Fig. 9, but the pin spacing determined earlier by DeltaE had to be modified to account for the fin spacing in the heat exchangers. The final pin spacing due to the physical dimensions of the exchanger was 746.8 μm pin center to pin center .

B. COMPARISON OF PIN STACK TO CONVENTIONAL STACK

Now that the pin spacing and diameter were firmly set, the computer comparisons of the pin stack and the conventional stack could now be more precisely handled. As before, the data obtained from Castro's experiments with the .82 cm heat exchanger at 27.6 kph mean pressure were used as the target output for the conventional stack. In this simulation the metal temperature of the two heat exchangers was fixed as well as the mean pressure. The average of the temperatures at the center and edge of the heat exchangers was used due to the temperature gradient observed across them in the previous experiment. The hot exchanger was set at 291 K and the cold heat exchanger temperature was held at 101 K. With these parameters the program was run and the length of the lower tube adjusted to meet the frequency measured previously. Figure 10 shows comparison of DeltaE results to the experimental data. Appendix A is a sample input file for DeltaE that contains all of the pertinent physical geometry.

The output matched the experiment within 10% and was considered to be close enough for a good simulation. Rather than vary the length of the lower tube to match the frequency at each pressure, at this point the physical geometry of the thermoacoustic engine was considered fixed and no more adjustments made. Therefore it is considered that this simulation will closely model Castro's experiments only around the 27.6 kph range. Despite this, the simulation is modeling a realistic thermoacoustic prime mover and the results drawn from this simulation should prove true in general.

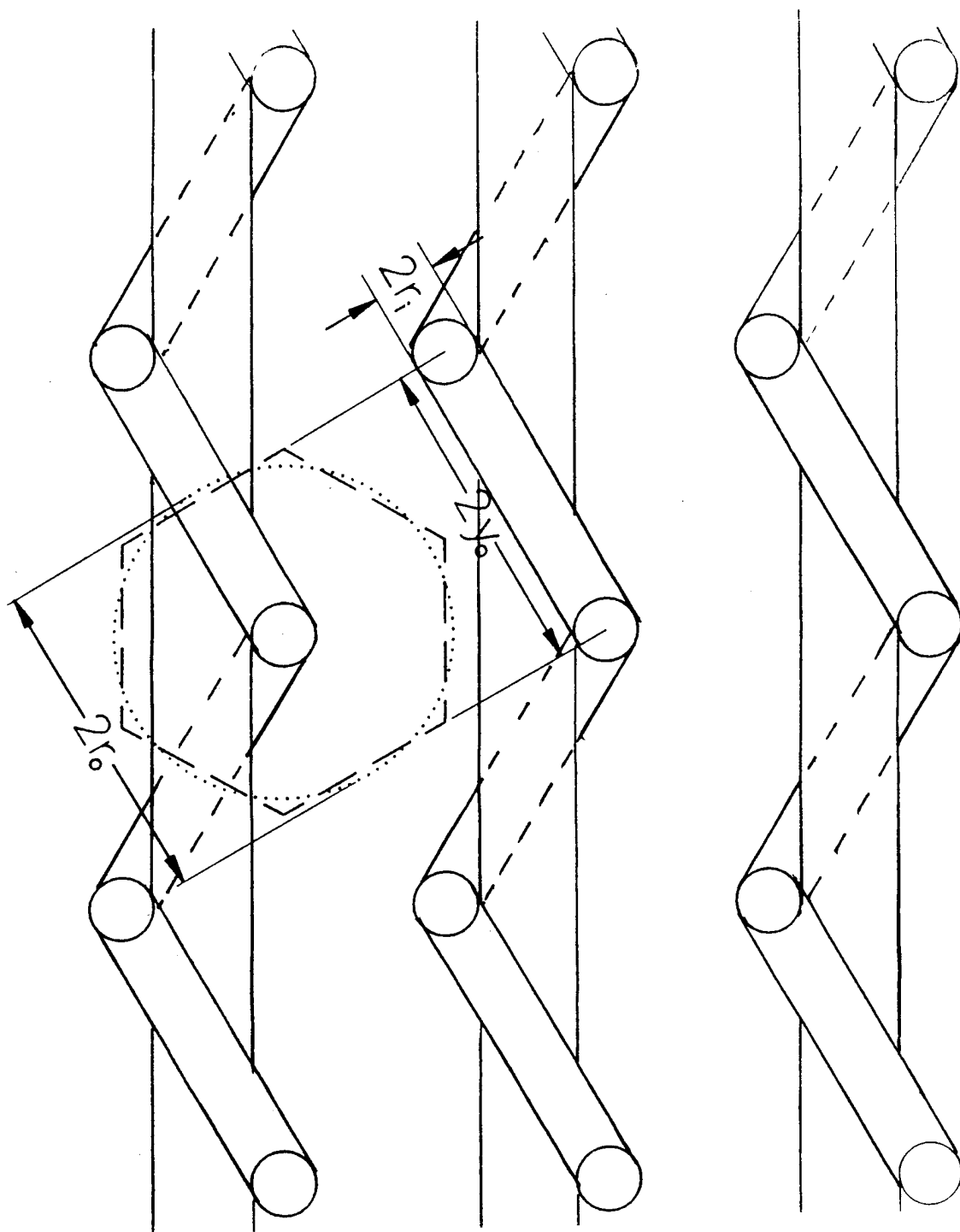


Figure 9. Geometry of a threaded heat exchanger.

DeltaE Results Compared to Experimental Data

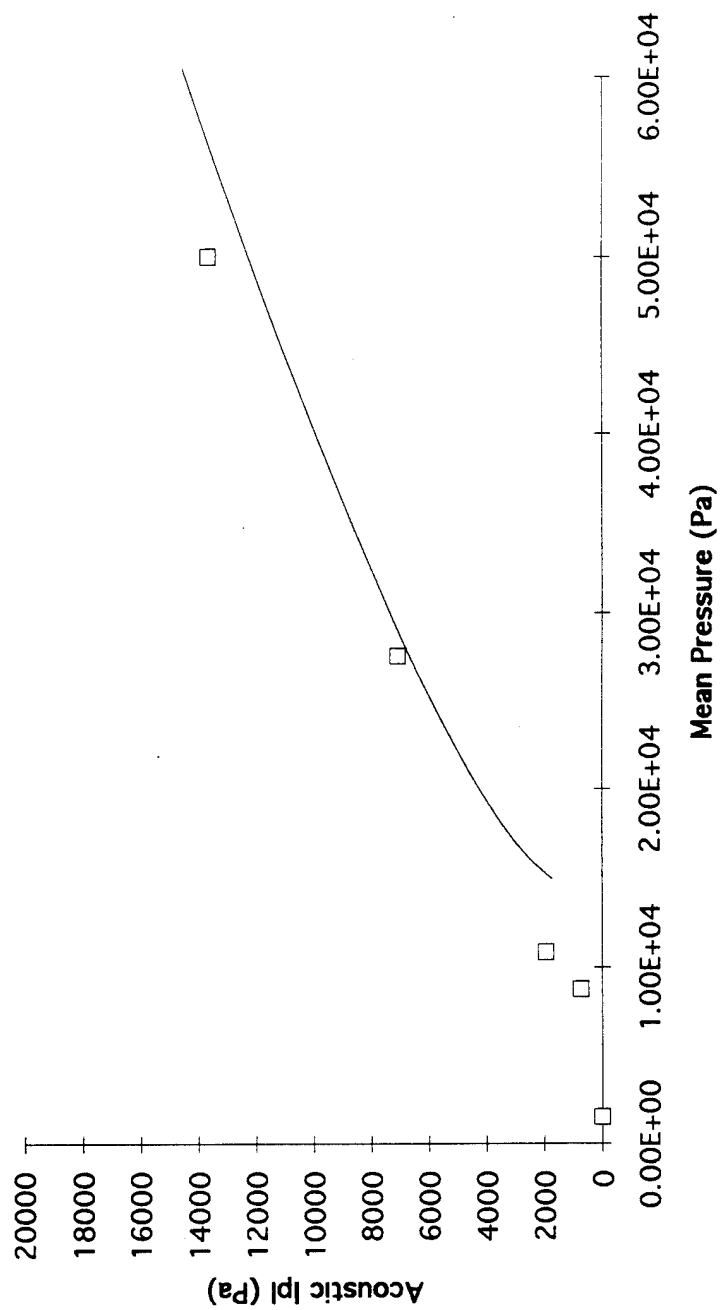


Figure 10. Comparison of DeltaE results to Castro's experimental data.

1. Varying Pressures

Now that the input file correctly described a conventional thermoacoustic engine, the performance of the two types of stacks could be examined. As before the temperatures were fixed for the hot and cold heat exchangers and the velocity was required to go to zero at the bottom end. The frequency, mean temperature of the fluid at the top end, heat provided to the engine and the acoustic output were allowed to vary. This simulation was run using different fixed mean pressures. For the conventional stack pressures from 15 kPa to 2.72 MPa were used, while the pin stack was operated over pressures from 8.96 kPa to .295 MPa. The pressure ranges were determined by the range at which DeltaE gave a reasonable solution, i.e. the solution converged. Results of all of these tests were tabulated and compared. Appendix B contains a sample input file for the pin stack using Castro's heat exchangers.

2. Onset

While normally defined as when the apparatus first generates sound, onset, in this case, is defined as the lowest pressure at which DeltaE gives a solution that converges. For the pin stack this occurred at 8.96 kPa, while for the more conventional rolled stack this occurred at 15 kPa. Figure 11 shows the acoustic pressure generated when varying the mean pressure. The pin stack reaching onset at a lower mean pressure and giving more acoustic pressure for given conditions is an indication that the pin stack geometry is beneficial at these pressures. The main advantage of the pin stack is to increase the ratio of the thermal effects to the viscous effects at penetration depths large compare to the pin radius. Also the surface area of the pins is about 1/5 of that of the plates which gives less area for the viscous effects to occur. This allows the running of the thermoacoustic prime mover a much mean lower pressure than before.

3. Efficiency

The efficiency, as defined by Eq. 10, is plotted as a percentage of Carnot efficiency for both the conventional and pin stacks in Fig. 12. Over the range from onset to .375 MPa the pin stack showed a dramatic improvement over that of the conventional rolled stack. The

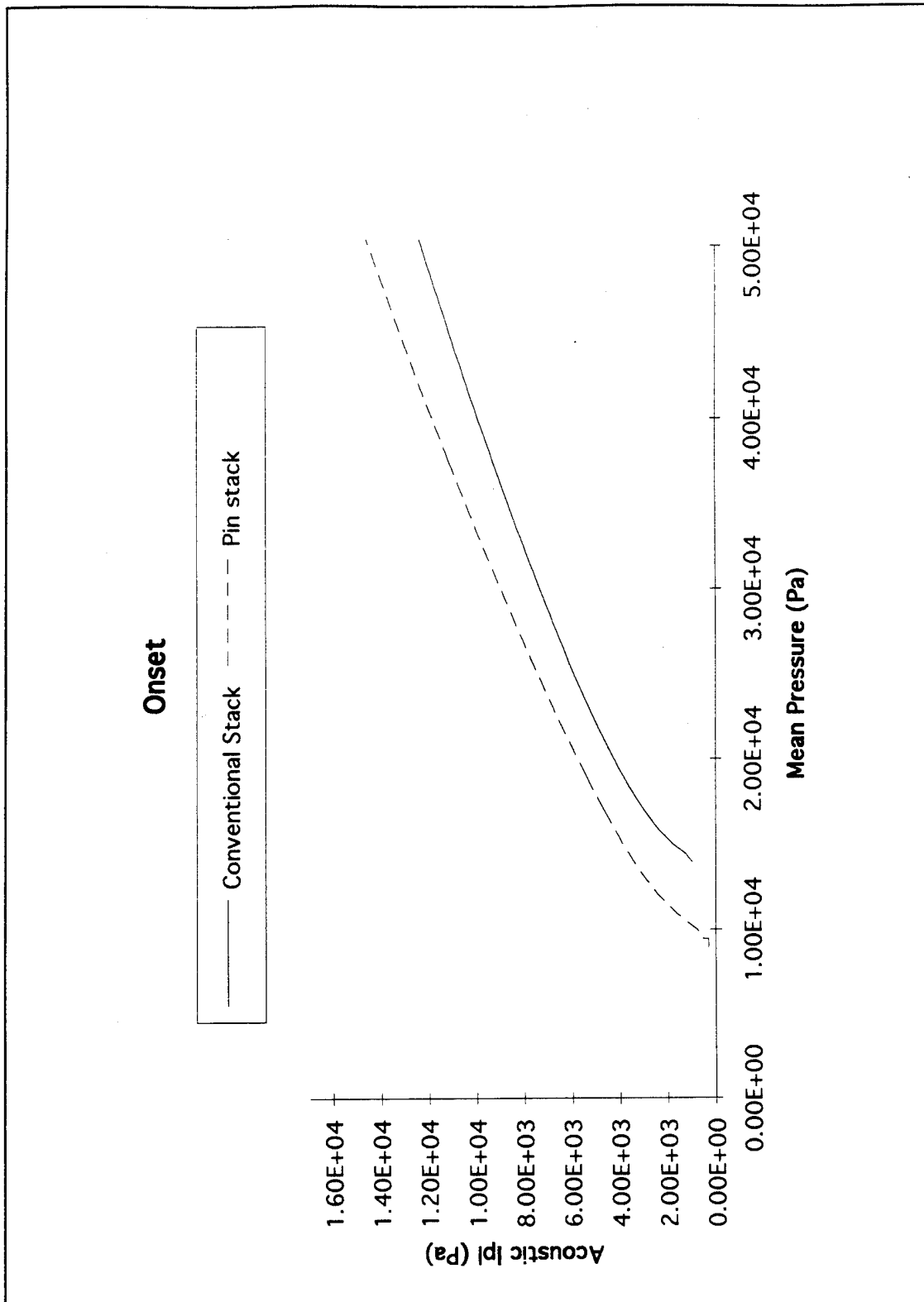


Figure 11. Comparison of onset for conventional and pin stacks.

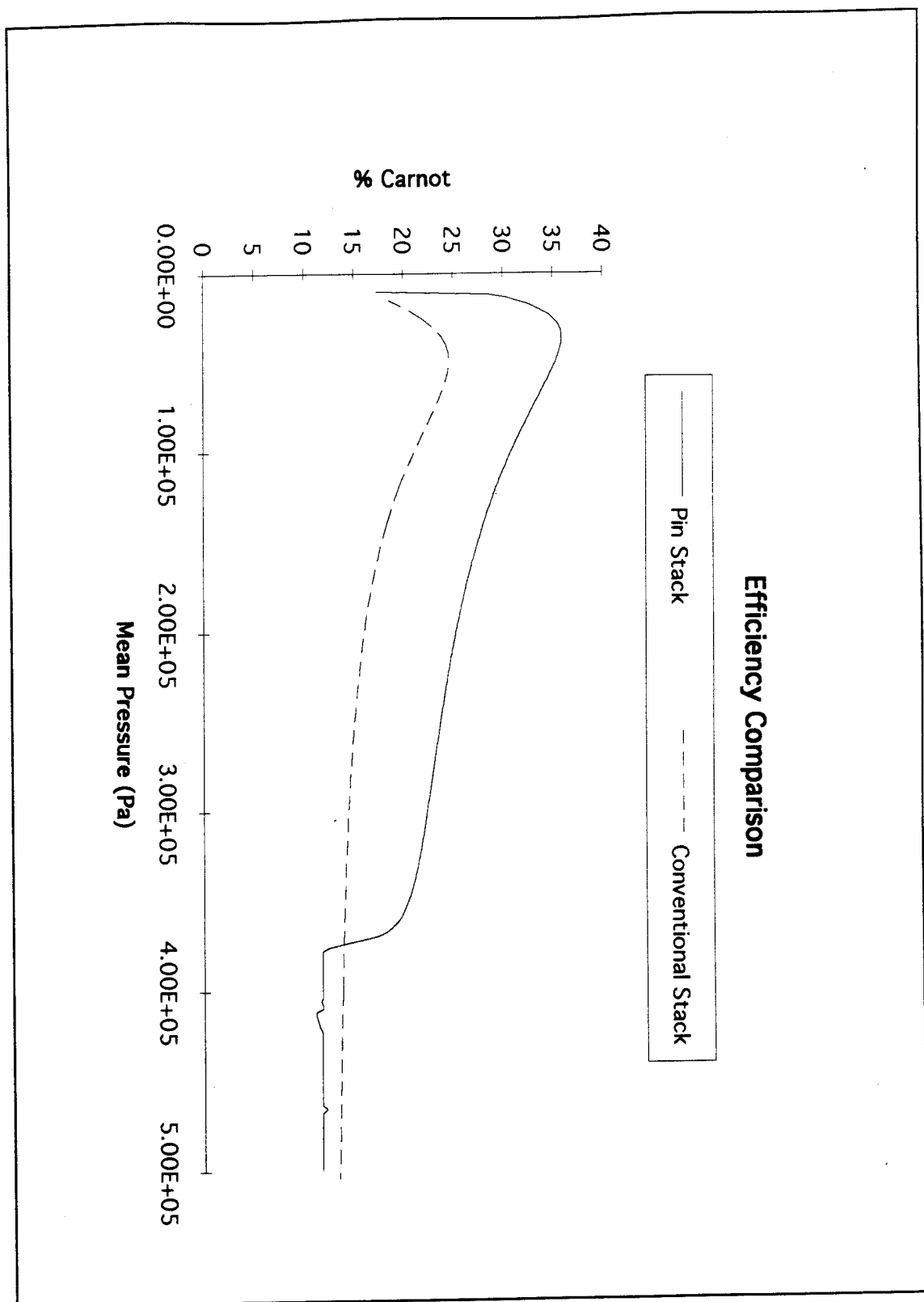


Figure 12. Comparison of efficiency of conventional and pin stacks.

maximum efficiency for the two stacks occurred at different mean pressures, 24% Carnot for the rolled stack and 36% for the pin stack, an improvement by a factor of 1.5. This efficiency improvement is a bit generous, however because it includes losses only in the stack. Total engine efficiency gains would approach these stack efficiency gains if other losses could be made small compared to the losses in the stack.

The magnitude of the thermal and viscous contributions to the work can be described by Rott's functions f_v and f_κ . The thermal effects are proportional to the Imaginary part of f_κ and the viscous losses proportional to $Im[f_v]/|1-f_v|^2$. (Swift, 1993) These functions are different for the pin and plate. For the pin, f_v or f_κ are given by

$$f_n = -\frac{\delta_n}{(i-1)} \frac{2r_i}{r_o^2 - r_i^2} \frac{Y_1[(i-1)r_o/\delta_n]J_1[(i-1)r_i/\delta_n] - J_1[(i-1)r_o/\delta_n]Y_1[(i-1)r_i/\delta_n]}{Y_1[(i-1)r_o/\delta_n]J_0[(i-1)r_i/\delta_n] - J_1[(i-1)r_o/\delta_n]Y_0[(i-1)r_i/\delta_n]}, \quad (12)$$

and for the plate they are given by

$$f_n = \frac{\tanh[(1+i)y_o/\delta_n]}{(1+i)y_o/\delta_n}, \quad (13)$$

where $n=v$ or κ . (Ward, 1993) Taking a ratio of the thermal effects to the viscous effects for both cases at the maximum efficiency points reveals that at the hot end of the stack the ratio is 1.42 for the pin and .484 for the conventional stack and at the cold end the ratio is 1.41 for the pins and .802 for the conventional. The higher ratio of the pins, almost a factor of 3 in the first case, results in the much higher efficiency.

The efficiency of the pin stack drastically rolls off at 3.75×10^5 Pa. This is believed to be due to the decrease in penetration depths. As the mean pressure goes up, the penetration depths go down. The volume of thermal effect and viscous effects start to decrease faster with the pin stack than with the rolled stack for the same reason the pin was more effective at low pressure. These effects go as the penetration depth squared. Combined with this, the smaller penetration depths mean these effects occur closer to the pin, so the

curvature of the pin becomes less important and the pin starts to look more like a plate to the gas. When this happens, the work performed on the fluid is dominated by the surface area of the stack. Since in this case the rolled stack has approximately five times the surface area, it can perform much more work on the fluid than the pin stack at these pressures. This shows a disadvantage of the pin stack - the operating range of mean pressures for a given geometry is reduced. The inefficiency reduction due to lessening of the penetration depths can be overcome by increasing the number of pins and keeping the spacing of the pins at about a δ_x apart. This will work until the penetration depths are so small the curvature of the pin no longer matters and the pin acts like a plate.

This effect of increasing the mean pressure also is easily seen by plotting the acoustic pressure vs. the mean pressure, Fig. 13. The pin stack produces more sound in the lower range but as the penetration depths decrease, less and less work is done on the fluid and the acoustic pressure starts to roll off. The conventional stack also shows the rolling off but at a much higher mean pressure because it is less sensitive to changes in the penetration depths.

4. Hysteretic Effects

While running the simulations for both stacks, hysteretic effects were noticed, as shown in Fig. 14. When running the simulation from low to high pressure in the 340-370 kph range, the engine produced more acoustic pressure than when running the simulation from high to low pressure. Hysteretic effects may be believable when the temperature gradient in the engine is examined. When the engine is producing large amounts of acoustic pressure the temperature gradient is highly dependent on the thermoacoustics. As less and less work is done on the fluid, the temperature gradient is more dependent on the wire and gas thermal conductivities. If the engine is started at a high pressure where the penetration depths are small, the engine will not have a substantial acoustic output until a favorable mean pressure and penetration depths are reached. At this point it may be possible that the thermoacoustic pumping of the heat increases the penetration depths and positively re-enforces the thermoacoustics. Likewise, if the engine is run and the mean pressure increased, the thermoacoustic pumping of the heat may maintain beneficial penetration depths over a much larger pressure range. This would increase the upper operating pressure of the pin stack.

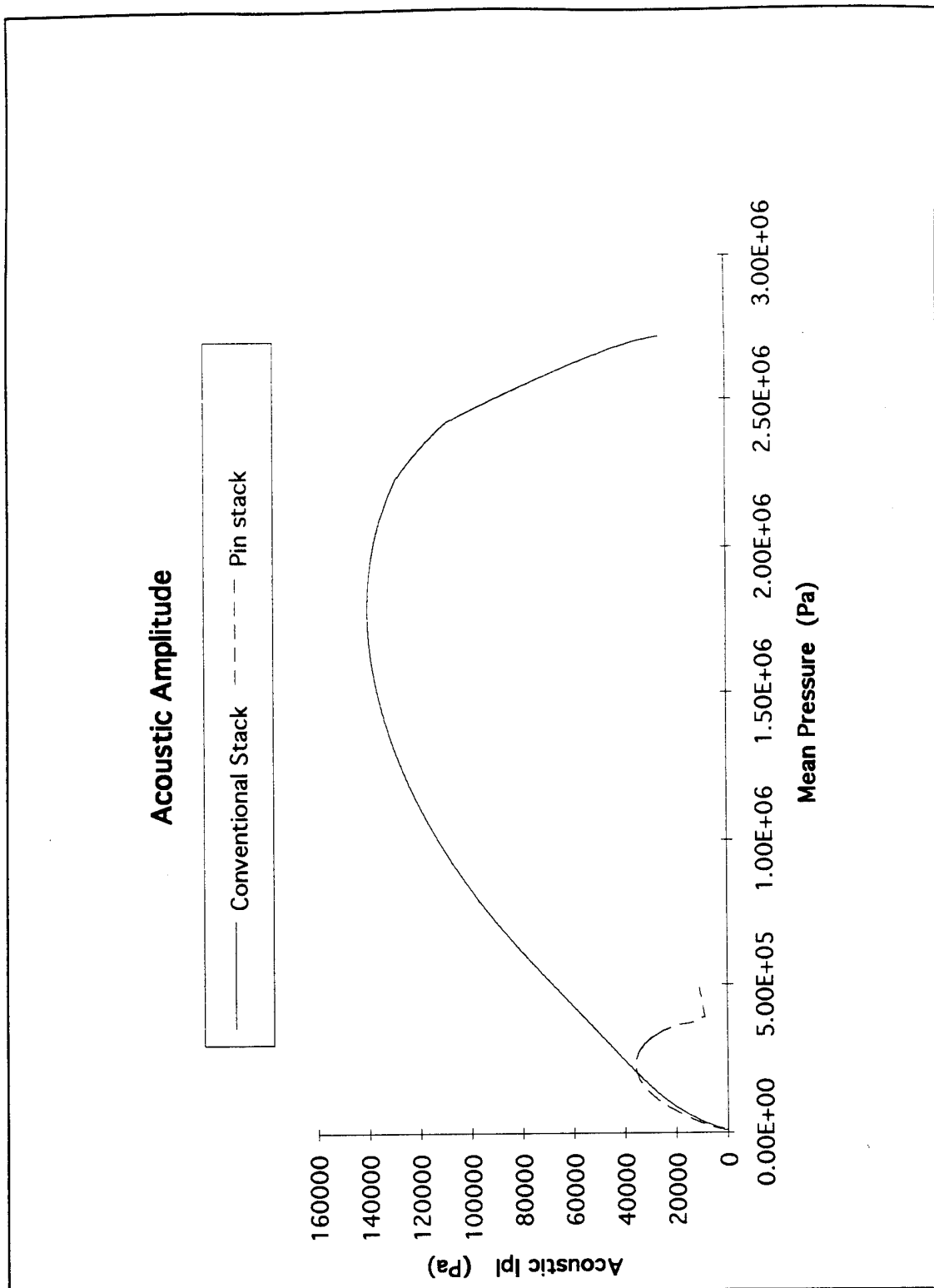


Figure 13. Comparison of acoustic amplitudes for conventional and pin stacks over a wide range of mean pressures.

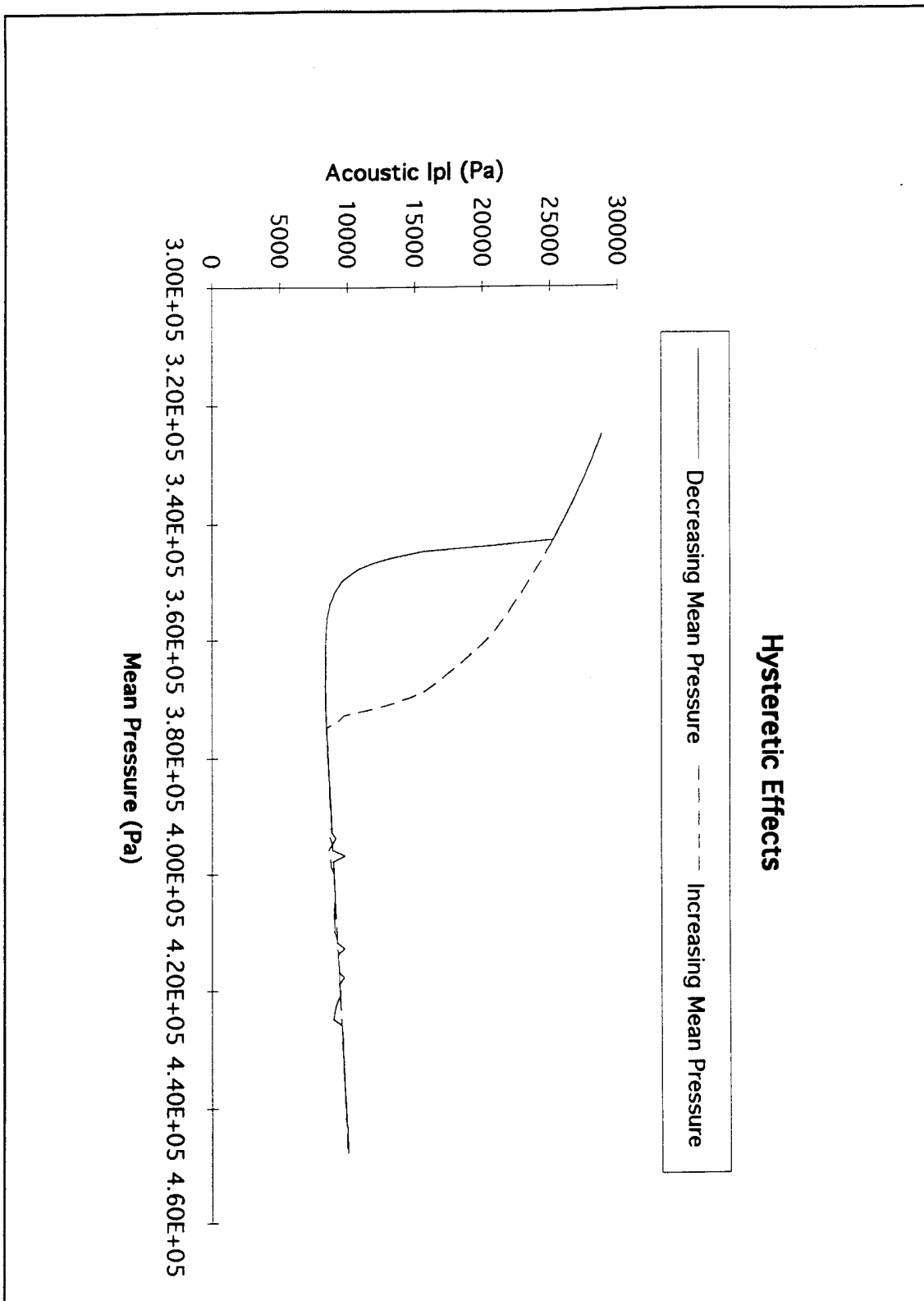


Figure 14. Hysteretic effects of the pins stack.

An examination of the thermoacoustic engine below onset should show the same type of effects. Below onset the temperature gradient is solely determined by the thermal conductivity of the fluid and pins when the temperature gradient finally reaches the critical temperature gradient and the thermoacoustics begin, the temperature gradient is then changed. This could explain why when operating engines around onset they tend cycle on and off. Around onset the thermoacoustics may tend to negatively influence the temperature gradient and shut off the engine. Since the pin stack is highly dependent on the curvature of the pins and the penetration depths of the fluid, these hysteretic effects are believed to be much more predominant than in the conventional rolled stack.

C. COMPUTER SIMULATIONS OF THE PROPOSED STACK

When running the simulations comparing the pin stack to the conventional stack, the same heat exchangers were used in both cases to ensure that just the stack geometries were being compared. The actual heat exchangers that will be used in making the pin stack, while similar, will have an effect on the performance of the engine. It was decided that running the actual geometry would provide curves that could be fit to actual data once the pin stack is operating and give some small insight into the effects of small changes in heat exchanger geometries to the pin stack. Appendix C lists a sample input file for the actual pin stack geometry. The differences between the two heat exchangers can be noted by comparing the heat exchanger segments in Appendix B to that in Appendix C. Castro's heat exchangers have plates that are .0292 cm thick and a plate gap of .0584 cm while the actual exchangers are .02303 cm thick with a plate gap of .0517 cm.

Using the same parameters as the previous simulations, this new geometry was run on DeltaE and the results compared to that using Castro's heat exchangers. Figures 15 and 16 show graphs of the acoustic amplitude and efficiency over a range of mean pressures.

Both curves are very similar. The actual heat exchangers yielded a slightly higher acoustic amplitude at lower pressures but at the cost of a lower efficiency. Onset was reached sooner by the Castro's exchangers than the actual ones, 8.6 kph to 9.5 kph. However, this

could just be an artifact of the computer simulation. The peak amount of acoustic amplitude for both geometries was the same but they reached their maximum at different mean pressures. Also, the proposed pin stack tended to roll off much sooner and steeper than the one using Castro's heat exchangers.

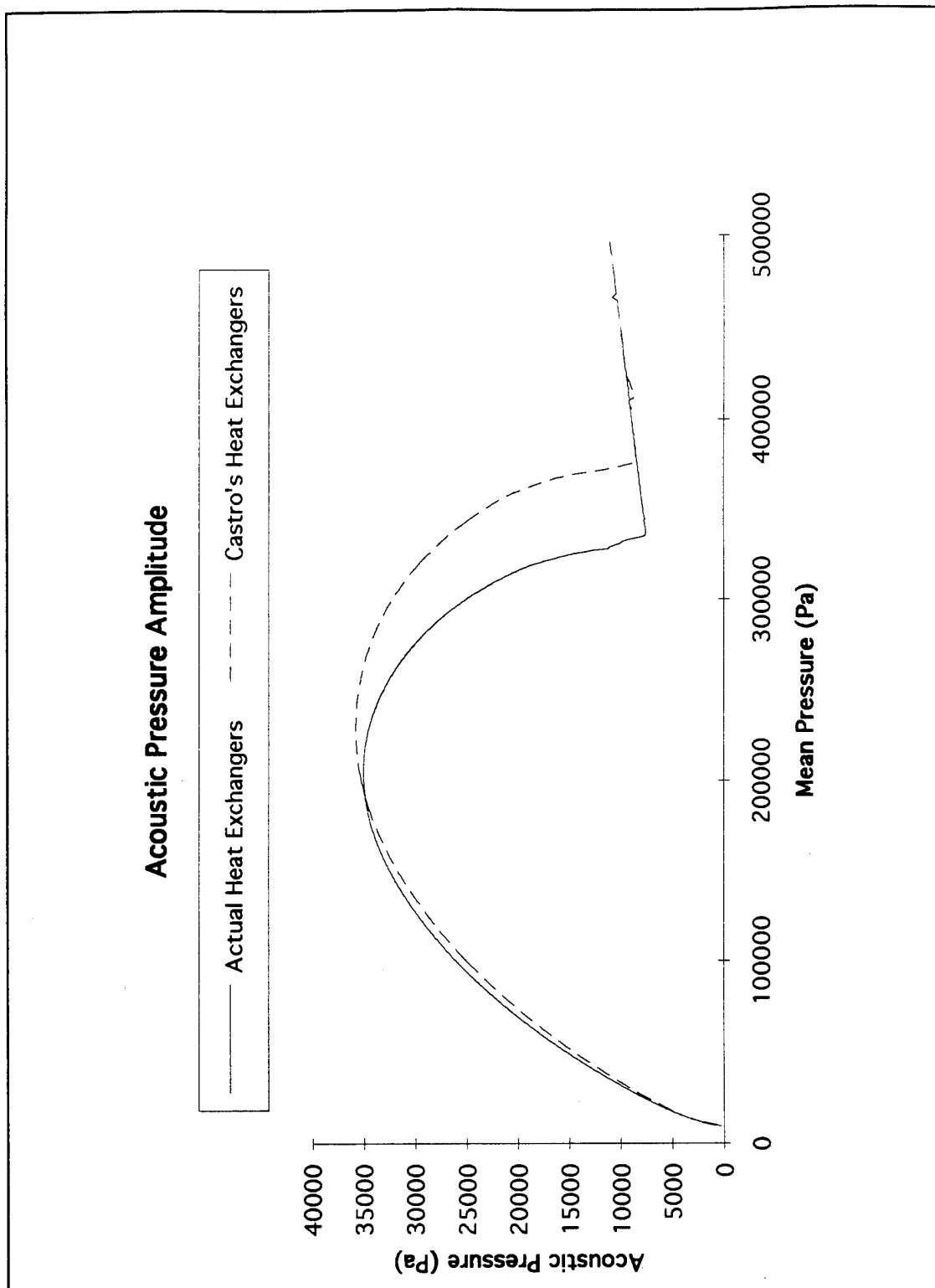


Figure 15. Comparison of acoustic amplitudes for two different heat exchanger pairs using the same pin geometry.

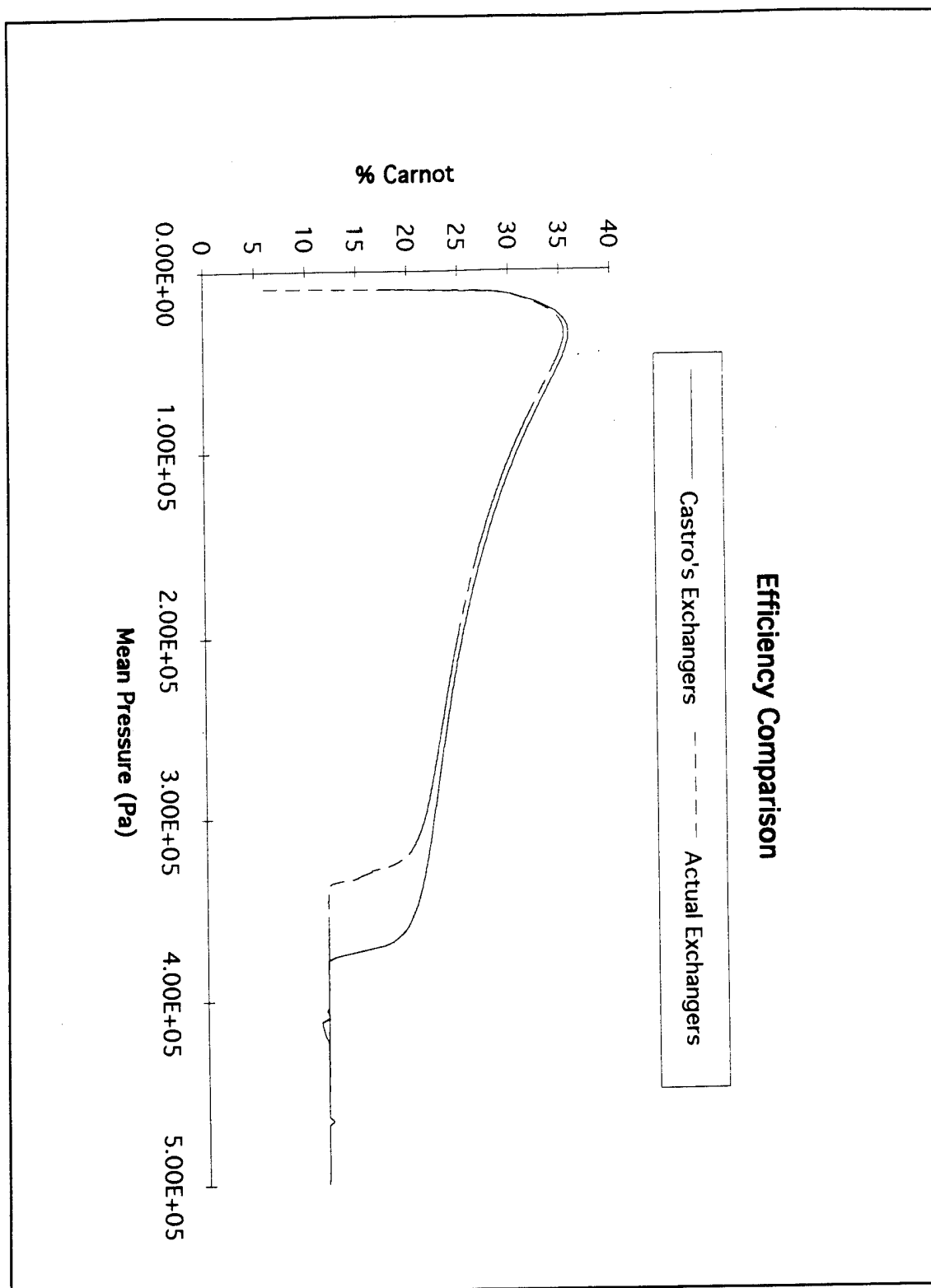


Figure 16. Comparison of efficiency between two different heat exchangers with the same pin geometry.

IV. CONSTRUCTION OF THE PIN STACK

Knowing the pin spacing and having the heat exchangers and wire on hand, the next step was to construct the pin stack. This was a multi-step trial and error process. Steps to make the pin stack are described below.

A. CREATION OF PIN STACK SHELL

The process of making the pin stack is divided into two sections. First the making of the pin stack shell, the stack without the pins, and second the insertion or winding of the pins. The testing of the stack shell was important for there must be an assurance that this part of the stack can withstand the temperature gradient placed upon it and can withstand the differential contraction due to the low temperatures before the daunting task of winding can even be addressed. Drawings of manufactured parts are given in Appendix D. The stack shell was constructed as described below.

1. Cutting The Heat Exchanger Notches

To keep the wires in proper spacing and position, it was determined that notches would be cut on the heat exchanger fins. Since the optimum spacing for the pins is in a hexagonal lattice, notches were cut into the fins at a 30° angle 508 μm deep, 152 μm wide and spaced 648 μm apart using a slitting saw on a mill. Careful consideration was made to ensure that the notches of one heat exchanger lined up with the other exchanger so that the stack wires would be along the acoustic axis of the tube.

2. Heat Exchanger Holders

Heat exchanger holders were constructed as shown in Appendix D (see D-1). The beveled edges allowed for easy soldering. The eight symmetric .437 cm holes were created to attach to like holes on the upper and lower tube of the thermoacoustic engine. The four recessed holes were created so that four 2/56 threaded rods could be used to support the weight of the lower pieces. Beleville Spring washers, measuring 1/8" ID x 1/4" OD x .0133", would help with the thermal contraction and expansion expected when operating at liquid nitrogen temperatures. The washers could exert a maximum force of 48 lbs apiece. The threaded rod was electrically isolated from the heat exchangers by the use of nylon washers.

This would allow the copper exchangers and the constantan wires to be used as a diagnostic pair of thermocouples, and keep thermal EMF's from driving currents between the wires and rods. The small lips seen on each of the heat exchanger holders were to fit around a piece of glass to hold it in place. Thermal contraction of the copper would bring it closer to the glass and ensure a good seal.

3. Insertion Of Glass

Glass was chosen as the material to separate the two heat exchangers and make the enclosure for the pins. Glass was desirable because of its insulating properties and it allowed viewing during the threading process. Viewing was necessary to ensure the pins were threaded correctly and not entwined. The glass was inserted inside the copper lips and secured using Armstrong A-12 epoxy. This epoxy chosen because it maintains its elasticity at low temperatures. Once this was assembled and allowed to cure the pieces were tested.

4. Initial Low Temperature Test

Since the stack would be operating at liquid nitrogen temperatures it was necessary to see how the assembled pieces would behave under these conditions before adding the pins. The stack, without the pins, was slowly inserted into a Dewar filled with liquid nitrogen and allowed to slowly cool by hanging in the vapor just above the liquid. Many disturbing high pitched "tinks" were heard from the stack. Once the piece was close to liquid nitrogen temperature it was then immersed in the liquid and allowed to come to liquid nitrogen temperature. The "tinks" accelerated into a crunching sound that ended with a bang. The piece was then removed and inspected. Inspection revealed that the copper had indeed contracted upon the glass but unfortunately more than desired and cracked the glass. A different method was designed to keep the glass in place.

5. Addition Of Teflon Seals

The copper lips were obviously not going to work so they were cut away. The epoxy and broken glass were also removed. Teflon seals were constructed by Robert Keolian to fit around the glass and into a groove cut into the heat exchange holders (see D-2). Using nuts on the threaded rod to adjust the tension, the spring washers provided the necessary pressure

to effect a seal between glass and copper. Once the glass was inserted and the seal established the new stack was tested in liquid nitrogen.

6. Second Low Temperature Test

This new stack shell was tested using the same method as described above. Only an occasional "tink" was heard. Inspection after immersion revealed that the Teflon did not noticeably crack the glass. The Teflon was observed to contract but the shape of the seal should maintain a good seal even with this contraction. Also the spring washers will absorb some of the contractions and expansions. Having a successful low temperature test, the next step was to insert the wires.

B. THREADING THE PINS BY HAND

Threading the wire between the two heat exchangers approximately 2300 times is a daunting task that should probably be done by using some sort of machine that would make both the exchangers and stack at the same time, especially for larger stacks. Keeping uniform tension in the wires, maintaining proper spacing and alignment are all problems that must be addressed when winding the stack.

The stack shell was mounted securely in a stand that had a base that could swivel. One end of a 1 m length of .003" (76 μ m) wire was threaded through a small 400 μ m OD, 10 cm long capillary tube that was used as a needle. The other end of the wire was attached to a heat exchanger fin using glue. Several glues and epoxies had been previously tested on a sample heat exchanger and dipped into liquid nitrogen to ensure it would hold. It was found that the glues that were thinner in consistency were difficult to work with in the small areas and tended to spread into areas, where glue was not desired. The epoxy took too long to dry to be of a lot of use. Krazy Glue Gel (Borden) was found to be most useful. The liquid nitrogen test showed that all the glues held but would give way if scraped or undue force was applied. It was decided that the glue joints would be made on the hot side if possible to avoid the harsh treatment of the liquid nitrogen.

Using a head mounted binocular magnifier, the 1 meter of wire was hand threaded back and forth between the exchangers many times, using the pattern show previously in Fig.

9, and the work examined. It was found that even with the high magnification and careful threading, the wires did not have even tension, in some cases would wrap around each other inside the glass tube, and the wire had many kinks and twists in it due to the large amount of manual manipulation. Since the experiment was to compare the pin stack to that of the conventional stack and the effects of treading defects is unknown it was decided that threading by hand was too unreliable for a method to threading. A jig is being developed that will give more exact tolerances.

V. CONCLUSIONS

The computer simulations lead to several results and an intuition about the construction of pin stacks. They also gave results that matched those from experiments already conducted using the conventional rolled stack. The pin stack reached onset at much lower mean pressure, produced higher acoustic amplitude, and over a significant mean pressure range the pin stack performed with a higher efficiency, up to 1.5 times the efficiency of a conventional stack. The pin stack, however, is much more sensitive to changes in penetration depths and more care must be taken when designing a pin stack. You lose with a pin stack for the same reason you win. The ratio of good thermal work volume to bad viscous loss volume goes as $(\delta_x/\delta_v)^2$ instead of δ_x/δ_v , but the good thermal work volume to *total* volume will also drop as δ_x^2 instead of δ_x , when δ_x gets to small. This loss in performance can be compensated for by including more pins and keeping the spacing at about a thermal penetration depth. However, when the penetration depths get very small compared to the pin radius, the pin stack gives very little advantage and starts to approach the results of a flat plate. Also, the comparison of the two heat exchanger geometries revealed that the heat exchangers will effect the performance of the pin stack, especially at high mean pressures. Each stack should be optimized for the given application by using computer simulations such as DeltaE.

Construction of a pin stack is nontrivial. When winding the wires by hand it is difficult, if not impossible, to keep the wires from kinking or twisting. The tolerances required are much more exacting than can be accomplished without a mechanical aide. Creating a jig to assist in the winding, however, is a time consuming process and the jig for the most part must be designed for a specific size of stack. Hand winding is impractical for large engines or for creating several pin stacks. A method must be designed that can mechanize the construction of the heat exchangers and pins as a unit which will allow for various sizes of heat exchangers and pins.

APPENDIX A. INPUT FILE FOR CONVENTIONAL STACK

This appendix contains the DeltaE input file for the conventional stack used in the simulations.

TITLE	Castro's Model	Conventional Stack	
BEGIN	Initial		0
2.760e4	a. Mean P	Pa	
167.	b. Freq	hz	
248.	c. T beg	K	
7.e3	d. p @0	Pa	
0.0	e. Ph (p) 0	deg	
0.0	f. U @0	m ² /s	
0.0	g. Ph(U)0	deg	
neon	Gas Type		
copper	Solid Type		

ENDCAP	Hot End		1
1.117e-3	a. Area m ²		
sameas 0	Gas Type		
copper	Solid Type		

ISODUCT	Hot Duct		2
sameas 1a	a. Area m ²		
0.118	b. Perimeter m		
7.308e-2	c. Length m		
sameas 0	Gas Type		
copper	Solid Type		

HXFRST	Hot Exchanger		3
sameas 1a	a. Area m ²		
0.667	b. GasA/A		
8.2e-3	c. Length m		
2.92e-4	d. y0 m		
10.0	e. Heat in W		
283.	f. Est-T K		
sameas 0	Gas Type		
copper	Solid Type		

STKSLAB	Conventional Stack	4
sameas 1a	a. Area m ²	
.75	b. Gas A/ A	
2.576E-2	c. Length m	
4.250e-4	d. y0 m	
5.000e-6	e. L plate m	
sameas 0	Gas type	
mylar	Solid Type	

HXLAST	Cold Exchanger	5
sameas 1a	a. Area m ²	
0.667	b. Gas A/A	
8.2e-3	c. Length m	
2.920e-4	d. y0	
-10.0	e. Heat in W	
106.	f. Est-T K	
sameas 0	Gas Type	
copper	Solid Type	

ISOCONE	assume straight cone from 1.485-1.250" -6	
sameas 1	a. Area	
sameas 2	b. Perimeter m	
2.055e-2	c. Length m	
7.917e-4	d. Area m ²	
9.975e-2	e. Perimeter m	
sameas 0	f. Gas	
copper	g. solid	

ISODUCT		7
sameas 6d	a. Area	
sameas 6e	b. Perimeter m	
.2699	c. Length	
sameas 0	d. Gas	
copper	e. solid	

ISOCONE		8
sameas 7	a. Area m ²	
sameas 7	b. Perimeter m	
1.252e-2	c. Length m	
1.966e-3	d. Area m ²	
0.157	e. Perimeter m	
sameas 0	Gas Type	
copper	Solid Type	

ISODUCT		9
sameas 8d	a. Area m ²	
sameas 8e	b. Perimeter m	
0.1930	c. Length m	
sameas 0	Gas Type	
copper	Solid Type	

ENDCAP Cold End		10
sameas 9a	a. Area m ²	
sameas 0	Gas Area	
copper	Solid type	

HARDEND Cold End		11
0.0	a. R(1/Z)	
0.0	b. I(1/Z)	
sameas 0	Gas Type	
copper	Solid Type	

APPENDIX B. INPUT FILE FOR PIN STACK

This appendix contains the sample input file for the pin stack simulations on DeltaE. Similar to Appendix A with Pin stack replacing the STKSLAB segment.

TITLE Pin Stack Model

!-----

BEGIN Initial 0
 2.760E+04 a Mean P Pa
 166. b Freq. Hz
 248. c T-beg K
 6.662E+03 d |p|@0 Pa
 .000 e Ph(p)0 deg
 .000 f |U|@0 m³/s
 .000 g Ph(U)0 deg

neon Gas type
 copper Solid type

!-----

ENDCAP Hot End 1
 1.117E-03 a Area m²
 sameas 0 Gas type
 copper Solid type

!-----

ISODUCT Hot Duct 2
 sameas 1a a Area m²
 .118 b perimeter m
 7.308E-02 c Length m
 sameas 0 Gas type
 copper Solid type

!-----

HXFRST Hot Exchanger 3
 sameas 1a a Area m²
 .667 b GasA/A
 8.200E-03 c Length m
 2.920E-04 d y0 m
 72.0 e Heat In W
 291. f Est-T K
 sameas 0 Gas type
 copper Solid type

!-----

STKPINS Pin Stack 4
 sameas 1a a Area m^2
 7.468e-4 b. 2yo
 2.58e-2 c. Length
 38.1e-6 d. Pin Radius
 sameas 0 e. Gas
 stainless f. Solid

!-----
 HXLAST Cold Exchanger 5
 sameas 1a a Area m^2
 .667 b GasA/A
 8.200E-03 c Length m
 2.920E-04 d y0 m
 -10.0 e Heat In W
 101. f Est-T K
 sameas 0 Gas type
 copper Solid type
 !-----

ISOCONE assume straight cone 6
 sameas 1a a Area Initial m^2
 sameas 2b b Perimeter Initial m
 2.860E-02 c Length m
 7.917E-04 d Area Final m^2
 9.975E-02 e Perimeter Finial m
 sameas 0 Gas type
 copper Solid type
 !-----

ISODUCT 7 7
 sameas 6d a Area m^2
 sameas 6e b Perimeter m
 .375 c Length m
 sameas 0 Gas type
 copper Solid type
 !-----

ISOCONE 8 8
 sameas 7a a Area m^2
 sameas 7b b Perimeter Initial m
 1.739E-02 c Length m
 1.966E-03 d Area Final m^2
 .157 e Perimeter finial m
 sameas 0 Gas type
 copper Solid type

```

!-----
ISODUCT 9 9
sameas 8d a Area m^2
sameas 8e b Perimeter m
.268 c Length m
sameas 0 Gas type
copper Solid type
!-----
ENDCAP Cold End 10
sameas 9a a Area m^2
sameas 0 Gas type
copper Solid type
!-----
HARDEND Cold End 11
.000 a R(1/Z)
.000 b I(1/Z)
sameas 0 Gas type
copper Solid type

```


APPENDIX C. INPUT FILE FOR ACTUAL PIN STACK

This contains the input file for the pin stack being built. This is similar to Appendix B with the exception of the heat exchanger geometry.

TITLE Geometry for manufactured pin stack

```
!-----
BEGIN      Initial      0
8.800E+03  a Mean P      Pa
148.       b Freq.      Hz   G
290.       c T-beg      K     G
763.       d |p|@0      Pa   G
.000       e Ph(p)0     deg
.000       f |U|@0      m^3/s
.000       g Ph(U)0     deg
neon       Gas type
copper     Solid type
```

```
!-----
ENDCAP     Hot End      1
1.117E-03  a Area       m^2
sameas 0   Gas type
copper     Solid type
```

```
!-----
ISODUCT     Hot Duct     2
sameas 1a   a Area       m^2
.118       b Perimeter   m
sameas 0   Gas type
copper     Solid type
```

```
!-----
HXFRST     Hot Exchanger 3
sameas 1a   a Area       m^2
.692       b GasA/A
8.200E-03  c Length     m
2.587-04   d y0        m
3.16       e Heat In    W
291.       f Est-T      K
sameas 0   Gas type
copper     Solid type
!-----
```

STKPINS Pin Stack 4
 sameas 1a a Area m^2
 7.468E-04 b 2 y0 m
 2.580E-02 c Length m
 3.810E-05 d R pin m
 sameas 0 Gas type
 stainless Solid type

HXLAST Cold Exchanger 5
 sameas 1a a Area m^2
 .692 b GasA/A
 8.200E-03 c Length m
 2.587E-04 d y0 m
 -10.0 e Heat In W
 101. f Est-T K
 sameas 0 Gas type
 copper Solid type

ISOCONE assume straight cone 6
 sameas 1a a Area m^2
 sameas 2b b Perimeter initial m
 2.860E-02 c Length m
 7.917E-04 d Area Final m^2
 9.975E-02 e Perimeter finial m
 sameas 0 Gas type
 copper Solid type

ISODUCT 7
 sameas 6d a Area m^2
 sameas 6e b Perimeter m
 .375 c Length m
 sameas 0 Gas type
 copper Solid type

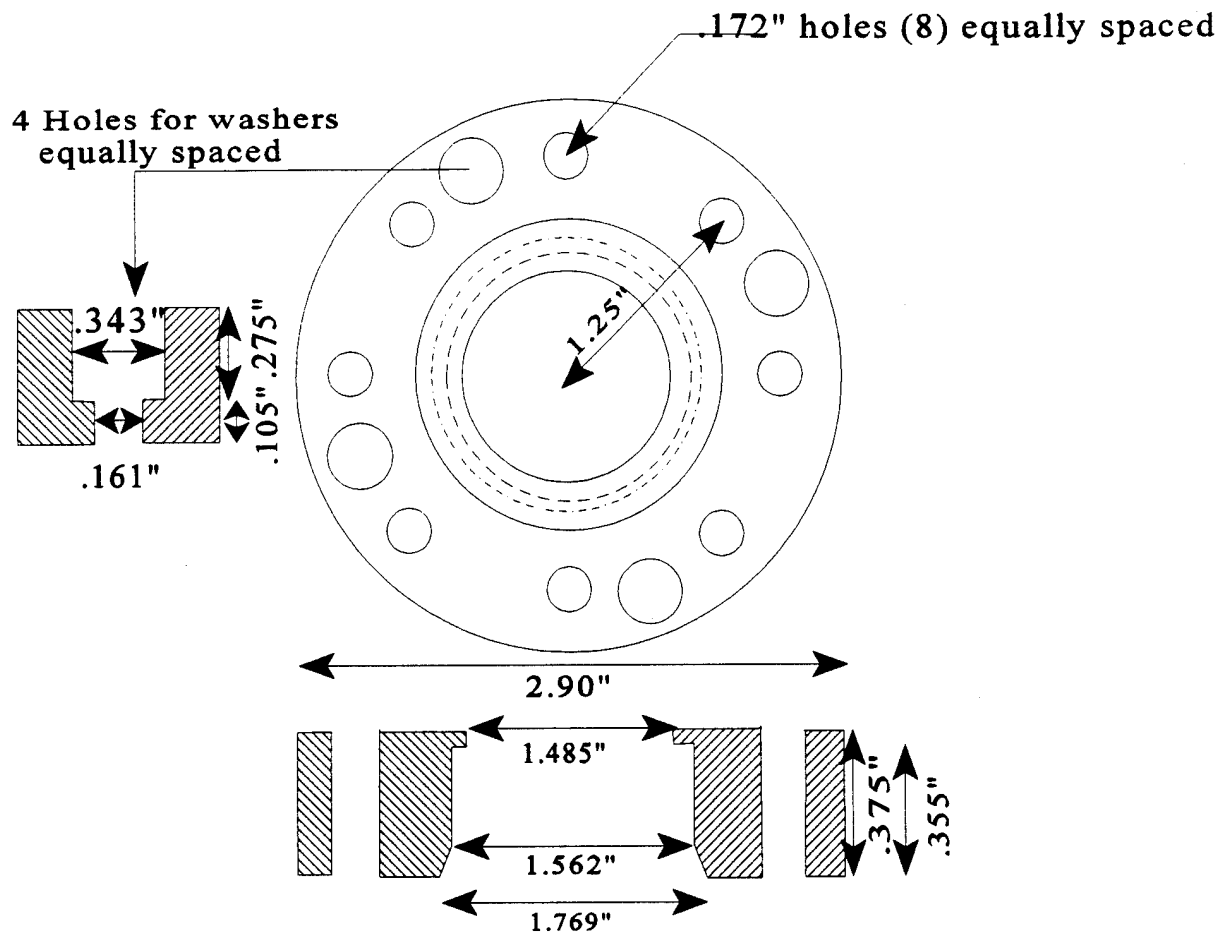
ISOCONE 8
 sameas 7a a Area m^2
 sameas 7b b Perimeter initial m
 1.739E-02 c Length m
 1.966E-03 d Area Final m^2
 .157 e Perimeter finial m
 sameas 0 Gas type
 copper Solid type

ISODUCT 9
 sameas 8d a Area m²
 sameas 8e b Perimeter m
 .268 c Length m
 sameas 0 Gas type
 copper Solid type

ENDCAP Cold End 10
 sameas 9a a Area m²
 sameas 0 Gas type
 copper Solid type

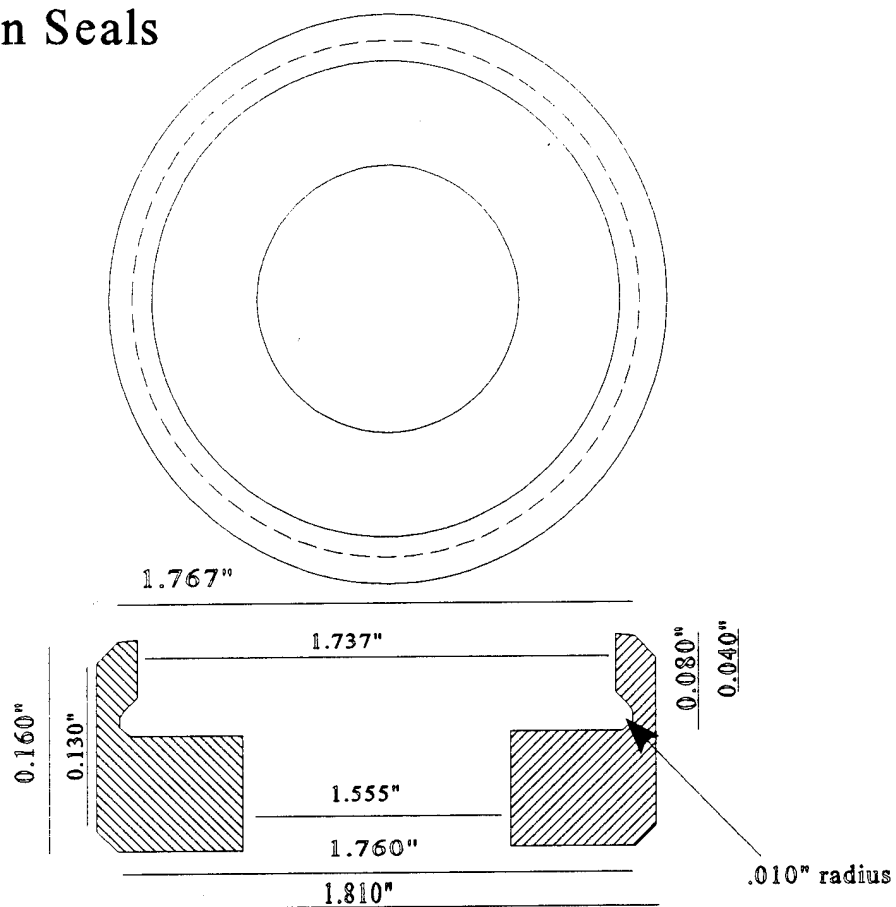
HARDEND Cold End 11
 .000 a R(1/Z)
 .000 b I(1/Z)
 sameas 0 Gas type
 copper Solid type

APPENDIX D. DRAWINGS FOR PIN STACK MANUFACTURE



D-1

Teflon Seals



D-2

LIST OF REFERENCES

Castro, N. C., Experimental Heat Exchanger Performance in a Thermoacoustic Prime Mover, Naval Postgraduate School, Monterey CA, Dec 1993.

Swift, G. W., "Thermoacoustic Engines," *J. Acoust. Soc. Am.*, vol. 84, 1145-1180, 1988.

Swift, G. W., Keolian, R. M., "Thermoacoustics in Pin-array Stacks," *J. Acoust. Soc. Am.*, vol. 94, pp. 941-943, August 1993.

Ward, W., Swift, G., "Design Environment for Low-amplitude Thermo-acoustic Engines," *J. Acoust. Soc. Am.*, vol. 95, pp. 3671,3672, 1994.

Ward, W., Swift, G., *Design Environment for Liner ThermoAcoustic Engines Deltae Tutorial and User's Guide*, Los Alamos National Laboratory, July 1993.

Wheatley, J. C., Swift, G. W., and Migliori, A., "The Natural Heat Engine," *Los Alamos Science*, Number 14, Fall 1986.

INITIAL DISTRIBUTION LIST

- | | |
|---|---|
| 1. Defense Technical Information Center
Cameron Station
Alexandria, Virginia 22304-6145 | 2 |
| 2. Library, Code 52
Naval Postgraduate School
Monterey, California 93943-5101 | 2 |
| 3. Robert M. Keolian
Dept. of Physics Code PH/Kn
Naval Postgraduate School
833 Dyer Rd. Rm 105
Monterey, California 93943-5117 | 2 |
| 4. Anthony A. Atchley
Dept. of Physics Code PH/Ay
Naval Postgraduate School
833 Dyer Rd. Rm 105
Monterey, California 93943-5117 | 1 |
| 5. F. Scott Nessler
15229 N th 52 nd Place
Scottsdale, Arizona 85254 | 2 |
| 6. Dr Jean Holmes
409 Avondale Dr
East Peoria, Illinois 61611 | 2 |
| 7. Dr Logan E Hargrove ONR 331
Office of Naval Research
800 North Quincy Street
Arlington Virginia 22217-5660 | 1 |
| 8. Director, Training and Education
MCCDC, Code C46
1019 Elliot Rd.
Quantico, Virginia 22134-5027 | 1 |